

A Nonparametric Approach to Augmenting a Bayesian VAR with Nonlinear Factors

Todd E. CLARK

Johns Hopkins University
and Federal Reserve Bank
of Cleveland
USA

Florian HUBER¹

University of Salzburg
Austria

Gary KOOP

University of Strathclyde
United Kingdom

Abstract

This paper proposes a Vector Autoregression augmented with nonlinear factors that are modeled nonparametrically using regression trees. There are four main advantages of our model. First, modeling potential nonlinearities nonparametrically lessens the risk of mis-specification. Second, the use of factor methods ensures that departures from linearity are modeled parsimoniously. In particular, they exhibit functional pooling where a small number of nonlinear factors are used to model common nonlinearities across variables. Third, Bayesian computation using MCMC is straightforward even in very high dimensional models, allowing for efficient, equation by equation estimation, thus avoiding computational bottlenecks that arise in popular alternatives such as the time varying parameter VAR. Fourth, existing methods for identifying structural economic shocks in linear factor models can be adapted for the nonlinear case in a straightforward fashion using our model. Exercises involving artificial and macroeconomic data illustrate the properties of our model and its usefulness for forecasting and structural economic analysis.

JEL: C11, C32, C53

KEYWORDS: Nonparametric VAR, nonlinear factor model, regression trees, macroeconomic forecasting, scenario analysis

¹The views expressed herein are solely those of the authors and do not necessarily reflect the views of the Federal Reserve Bank of Cleveland or the Federal Reserve System. Please address correspondence to: Florian Huber. Department of Economics, University of Salzburg. *Address:* Mönchsberg 2a, 5020 Salzburg, Austria. *Email:* florian.huber@plus.ac.at.

1 Introduction

Researchers in macroeconomics and finance routinely work with high dimensional time series data sets involving dozens or hundreds of variables. Vector Autoregressions (VARs), dynamic or static factor models (DFMs or SFMs) and combinations of the two (e.g., factor augmented VARs or FAVARs) are commonly used. VARs are particularly popular since they often forecast better than factor models (see, among many others, [Bańbura, Giannone, and Reichlin, 2010](#)) and a well-developed set of tools exist for carrying out structural economic analysis (e.g., calculating impulse response functions). Bayesian methods are popular in these large, often over-parameterized, models since prior shrinkage can help reduce the problem of over-fitting. Bayesian inference in these models typically proceeds using computationally demanding Markov chain Monte Carlo (MCMC) methods.

Even in the linear, homoscedastic VAR or factor model worlds, computational and over-fitting issues can be substantial when the number of variables under study is large (see, e.g., the discussion of VAR computation in [Carriero, Clark, and Marcellino, 2019](#)). These problems become greatly magnified in the nonlinear world. Even when the form of nonlinearity is known, incorporating it into a parametric nonlinear VAR can lead to a very non-parsimonious and over-parameterized model. For instance, with VARs, it is common to allow nonlinearities in the form of time-varying parameters (TVP), under which coefficients continuously evolve as random walks. However, carrying out Bayesian inference in a TVP-VAR with as many as 100 variables is a huge computational challenge. Furthermore, in any macroeconomic or financial data set there are so many empirically plausible nonlinearities that might occur that the researcher who adopts any particular parametric model (e.g., a TVP-VAR or a Markov switching DFM) runs a risk of misspecification.

These considerations motivate the high-dimensional nonlinear time series model we propose in this paper. For reasons detailed below, we view the model and our estimation approach as effectively balancing — in a new way relative to existing options — tradeoffs associated with over-parameterization, misspecification, and computation. One component of the model is simply a linear VAR. Nonlinearities are modeled as deviations from

this linear model. It is more flexible than a parametric model in that the nonlinearities are modeled nonparametrically using regression trees. We ensure parsimony by assuming a factor structure for the nonlinear part of the model. We use the term functional pooling for this since information is pooled across the variables so as to improve estimation of the nonlinear functions determining the factors.

Computational gains arise because a small number of factors drive the nonlinearity of all the observable series. In particular, conditional on these factors, the errors in the linear VAR part of the model take a static factor model form which allows for equation-by-equation estimation of the VAR block, greatly reducing the computational burden. Thus, the factor structure we adopt means that our model is scalable and can be used for structural inference through sign restrictions along the lines of [Baumeister and Hamilton \(2015\)](#) and [Korobilis \(2022\)](#).

To provide additional motivation for our model, note that there are reasons to think that macroeconomic data is driven by a small number of fundamental shocks (see, e.g., [Bai and Ng, 2007](#); [Forni, et al., 2025](#)). Furthermore, in the TVP-VAR literature where TVPs are assumed to evolve according to random walks, papers such as [Chan, Eisenstat, and Strachan \(2020\)](#) use random walk factor structures which reduce the number of processes driving the time-varying parameters. Thus, the empirical regularity that there is often a high degree of commonality in time varying parameters can be exploited to ensure a greater degree of parsimony. Our model exploits this regularity, but in a more flexible, nonparametric way. Our model can also be seen as a more general specification for capturing nonlinearities such as the time dependency of VAR coefficients in [Kim, Matthes, and Phan \(2025\)](#) that is related to the smooth transition specifications cited in that study.

In the paper’s empirical analysis, we apply our proposed nonparametric nonlinear VAR-factor model for macroeconomic forecasting key US aggregates and structural analysis of the impacts of monetary policy shocks. The forecasting application shows noticeable gains in the accuracy of out-of-sample density forecasts compared to a linear VAR, especially for alternative measures of aggregate inflation. The structural application, which uses sign restrictions for identification, uncovers significant nonlinearities — i.e., asymmetries in impacts — in responses of most of the indicators of economic activity and

inflation considered. With large shocks to monetary policy, tightenings (increases of the funds rate) have bigger impacts in absolute value than easings of policy.

The paper proceeds as follows. Section 2 presents our proposed model and provides a high-level overview of the estimation algorithm. Section 3 provides Monte Carlo evidence on the ability of the model to uncover various types of nonlinearity in common factors. Sections 4 and 5 provide application results on, respectively, out-of-sample forecasting and structural analysis. Section 6 summarizes and concludes. An Online Appendix provides additional details on data, estimation, and some empirical results.

2 Econometric framework

In this section, we first develop and motivate our model before discussing Bayesian estimation and inference in it. Our specification amounts to adding nonlinear factors, modeled using BART, to a linear VAR and hence we refer to our model as the factor-BART VAR.

2.1 The factor-BART VAR

Our aim is to model a M –dimensional vector \mathbf{y}_t that includes macroeconomic and financial variables with a flexible multivariate time series model. Existing nonlinear models (see Primiceri, 2005; Cogley and Sargent, 2005; Sims and Zha, 2006; D’Agostino, Gambetti, and Giannone, 2013; Huber and Rossini, 2022; Huber, et al., 2023, among many others) have the shortcoming that they do not scale well to large dimensions and are prone to overfitting. The factor BART model of Velasco (2025) is particular noteworthy as it adopts the use of BART methods for modeling factors, but in a different manner to our factor-BART VAR. The factor BART model has the number of BART functions being of the same dimension as the number of variables in the model, thus involving estimation of M BART functions. This contrasts with our functional pooling approach which involves a small number of BART functions.²

²In addition, the approach of Velasco (2025) differs from ours in that the model of Velasco (2025) assumes the nonlinearities appear in the measurement equation relating the data of interest to the factors, whereas our model assumes the nonlinear factors appear in the transition dynamics for the data series of

Prior regularization in all these high dimensional models is very useful in reducing the risk of over-fitting, but imposing restrictions can also help if these restrictions are empirically or theoretically justified. This is the path we explore in the present paper using a nonlinear factor structure. There is evidence that nonlinearities in \mathbf{y}_t might be similar across groups of variables. For instance, series that measure economic output might feature a similar dependence on nonlinear factors. This provides the motivation to design a model that induces nonlinear features on groups of variables (as opposed to on each variable individually). The factor-BART VAR assumes that \mathbf{y}_t evolves according to the following nonparametric model:

$$(1) \quad \mathbf{y}_t = \mathbf{A}\mathbf{x}_t + \mathbf{\Lambda}_f \mathbf{f}_t + \boldsymbol{\varepsilon}_t,$$

where \mathbf{A} is a $M \times K (= Mp)$ matrix that linearly links \mathbf{y}_t to its p lags, stored in $\mathbf{x}_t = (\mathbf{y}'_{t-1}, \dots, \mathbf{y}'_{t-p})'$. We assume that the shocks in $\boldsymbol{\varepsilon}_t$ are Gaussian with a covariance matrix $\boldsymbol{\Sigma}_\varepsilon$. Specific assumptions about $\boldsymbol{\Sigma}_\varepsilon$ will be discussed below.

Nonlinear dynamics are introduced through a sequence of Q_f latent factors with nonlinear state equation:

$$(2) \quad \mathbf{f}_t = \boldsymbol{\mu}(\mathbf{x}_t) + \mathbf{w}_t, \quad \mathbf{w}_t \sim \mathcal{N}(\mathbf{0}_{Q_f}, \mathbf{V}_f).$$

The mean of the factors is given by $\boldsymbol{\mu}(\mathbf{x}_t) = (\mu_1(\mathbf{x}_t), \dots, \mu_{Q_f}(\mathbf{x}_t))'$, where each component function $\mu_j : \mathbb{R}^K \rightarrow \mathbb{R}$ takes \mathbf{x}_t as input and returns a scalar output. The $M \times Q_f$ coefficient matrix $\mathbf{\Lambda}_f$ then maps the factors back into the observed series. A key point to note here is that the functional form of $\mu_j(\mathbf{x}_t)$ and $\mu_i(\mathbf{x}_t)$ can differ. The loadings $\mathbf{\Lambda}_f$ are then used to weight each of the functions such that the dynamics for a particular variable are best explained. To understand this more clearly, observe the s^{th} equation from Eq. (1). By substituting Eq. (2), it becomes evident that:

$$(3) \quad y_{st} = \mathbf{a}'_s \mathbf{x}_t + \lambda_{f,s1} \mu_1(\mathbf{x}_t) + \dots + \lambda_{f,sQ_f} \mu_{Q_f}(\mathbf{x}_t) + \tilde{\varepsilon}_{st},$$

interest.

with \mathbf{a}_s denoting the s^{th} row of \mathbf{A} , $\lambda_{f,sj}$ denotes the $(s,j)^{th}$ element of $\mathbf{\Lambda}_f$ and $\tilde{\varepsilon}_{st} = \sum_{j=1}^{Q_f} \lambda_{f,sj} w_{jt} + \varepsilon_{st}$ is a shock term where w_{jt} denotes the j^{th} element of \mathbf{w}_t and ε_{st} denoting element s of the shock vector $\boldsymbol{\varepsilon}_t$. This equation also illustrates that our model can be interpreted as a nonlinear VAR with Q_f static factors \mathbf{w}_t .³ If we set $\boldsymbol{\Sigma}_\varepsilon$ to a diagonal matrix, the factors in \mathbf{w}_t would control the contemporaneous relations across shocks in $\tilde{\boldsymbol{\varepsilon}}_t = (\tilde{\varepsilon}_{1t}, \dots, \tilde{\varepsilon}_{Mt})'$.

This specification nests two special cases. First, if $\lambda_{f,s1} = \dots = \lambda_{f,sQ_f} = 0$ we end up with a linear regression model for equation s . This observation allows us to design a Bayesian shrinkage prior that allows for a data-based assessment of whether nonlinear features are necessary. Second, if we set $\mathbf{\Lambda}_f = \mathbf{I}_M$ (and thus set $Q_f = M$) we end up with the mixBART specification proposed in Clark, et al. (2023). Relative to the latter model our proposed specification is very parsimonious because instead of having to estimate M different functions we only need to estimate $Q_f (\ll M)$ functions. If $M = 100$ and $Q_f = 5$, we are estimating only five unknown functions instead of 100, reducing functional complexity by 95%. This assumption is motivated by the fact that if series display similar forms of nonlinearities (such as different measures of aggregate inflation or subcomponents of GDP) it makes sense to introduce structure on the functional relationship and we achieve this through the factor specification which leads to function pooling.

We illustrate how function pooling works through three simple examples. All three analytical examples assume $M = 3$ observed time series and $Q_f = 2$ latent nonlinear factors so that $\boldsymbol{\mu}(\mathbf{x}_t) = (\mu_1(\mathbf{x}_t), \mu_2(\mathbf{x}_t))'$.

Example 1. Consider the following matrix of factor loadings:

$$\mathbf{\Lambda}_f = \begin{bmatrix} 1 & 0 \\ 1 & 0 \\ 0 & 1 \end{bmatrix} \quad \text{then} \quad \mathbf{\Lambda}_f \boldsymbol{\mu}(\mathbf{x}_t) = \begin{bmatrix} \mu_1(\mathbf{x}_t) \\ \mu_1(\mathbf{x}_t) \\ \mu_2(\mathbf{x}_t) \end{bmatrix}.$$

³Baumeister, et al. (2025), in a dynamic panel model, assume that a single factor determines the nonlinearities with respect to a set of aggregate macroeconomic series and assume that observed characteristics determine the loadings associated with this factor.

This example implies that series 1 and 2 share the same nonlinear function $\mu_1(\mathbf{x}_t)$, while the third series depends on a separate nonlinear function $\mu_2(\mathbf{x}_t)$. This setup captures common nonlinear behavior among subsets of series.

Example 2. Now assume:

$$\mathbf{\Lambda}_f = \begin{bmatrix} 1 & 0 \\ 0 & 1 \\ 0 & 0 \end{bmatrix}, \quad \text{then} \quad \mathbf{\Lambda}_f \boldsymbol{\mu}(\mathbf{x}_t) = \begin{bmatrix} \mu_1(\mathbf{x}_t) \\ \mu_2(\mathbf{x}_t) \\ 0 \end{bmatrix}.$$

Series 1 and 2 each have their own nonlinear functions, while series 3 exhibits only linear dynamics. The model flexibly allows for nonlinearities to be omitted when not supported by the data.

Example 3. Finally, suppose:

$$\mathbf{\Lambda}_f = \begin{bmatrix} 0.5 & 0.5 \\ 0.5 & -0.5 \\ 0 & 1 \end{bmatrix}, \quad \text{then} \quad \mathbf{\Lambda}_f \boldsymbol{\mu}(\mathbf{x}_t) = \begin{bmatrix} 0.5\mu_1(\mathbf{x}_t) + 0.5\mu_2(\mathbf{x}_t) \\ 0.5\mu_1(\mathbf{x}_t) - 0.5\mu_2(\mathbf{x}_t) \\ \mu_2(\mathbf{x}_t) \end{bmatrix}.$$

All three series depend on the same two latent functions, but through different linear combinations. This introduces complex nonlinear structure while maintaining parsimony if each μ_j takes a simple form.

2.2 Modeling the error variance and approximating the unknown functions

Two components of our model still require discussion. First, the error variance $\boldsymbol{\Sigma}_\varepsilon$. For this, we introduce a factor model so that:

$$(4) \quad \boldsymbol{\Sigma}_\varepsilon = \mathbf{\Lambda}_q \mathbf{V}_q \mathbf{\Lambda}_q' + \boldsymbol{\Omega},$$

with $\mathbf{\Lambda}_q$ denoting a $M \times Q_q$ matrix of factor loadings, \mathbf{V}_q is a $Q_q \times Q_q$ diagonal matrix of factor variances and $\boldsymbol{\Omega} = \text{diag}(\omega_1^2, \dots, \omega_M^2)$ is a diagonal matrix of measurement error

variances. Notice that Eq. (4) means the innovation term of the model can be equivalently written as:

$$(5) \quad \boldsymbol{\varepsilon}_t = \boldsymbol{\Lambda}_q \mathbf{q}_t + \boldsymbol{\eta}_t, \quad \boldsymbol{\eta}_t \sim \mathcal{N}(\mathbf{0}, \boldsymbol{\Omega}), \quad \mathbf{q}_t \sim \mathcal{N}(\mathbf{0}, \mathbf{V}_q),$$

where \mathbf{q}_t are zero mean static factors. This representation shows that the reduced-form errors of the model can be decomposed into a common component $\boldsymbol{\Lambda}_q \mathbf{q}_t$ and a sequence of idiosyncratic measurement errors. If we wish to use the model for structural inference, restrictions can be used on $\boldsymbol{\Lambda}_q$ to identify the factors in \mathbf{q}_t as fundamental economic shocks as in Korobilis (2022).

Second, we approximate the functions μ_i through Bayesian additive regression trees (BART Chipman, George, and McCulloch, 2010). BART is a sum-of-trees model which approximates:

$$(6) \quad \mu_i(\mathbf{x}_t) \approx \sum_{s=1}^S \mathbf{t}(\mathbf{x}_t | \mathbf{m}_{i,s}, \mathcal{T}_{i,s}),$$

where \mathbf{t} is a tree function, $\mathbf{m}_{i,s}$ a vector of terminal node parameters and $\mathcal{T}_{i,s}$ a tree structure. These tree structures consist of decision rules that take the form $\{x \leq c\}$ or $\{x > c\}$ and hence split the input space defined by x up into a sequence of disjoint sets. For each of these disjoint sets, there is a terminal node parameter which plays the role of a fitted value in a regression model. Trees are prone to overfitting if no regularization is introduced. Summing over many (possibly) complex trees further increases the risk of overfitting. As a solution, BART uses Bayesian regularization priors to force each of the trees to take a particularly simple form and thus act as a weak learner. Summation over many of such simple trees produces a model with a great deal of representation flexibility, while regularization to keep the trees simple limits the risk of overfitting.

The factor-BART VAR is capable of capturing a wide range of possible nonlinear relations through the factor structure. As noted in the preceding examples, one possible model formulation could feature common nonlinear behavior among subsets of the data series included in the model, with most series sharing the same nonlinear function while

one or a few series depend on a separate nonlinear function. Alternatively, the nonlinear factor structure might not be full rank, with all series depending on the same, small number of latent functions but through different linear combinations. In yet other options (employed in our Monte Carlo simulations presented in the next section), the model might feature (i) nonlinearities arising with threshold effects, so that above and below a certain threshold, the dynamics of the common factors are governed by different sets of coefficients, or (ii) factors that are governed by highly nonlinear functions, such as trigonometric functions. As this discussion suggests, an advantage of using BART or other nonparametric methods is that the range of nonlinear forms it is capable of modeling is enormous. In contrast, [Guerrón-Quintana, Khazanov, and Zhong \(2023\)](#) is an example of a nonlinear dynamic factor model where the nonlinearities involve a particular quadratic form. They show how their model relates closely to a nonlinear DSGE model. Quadratic forms such as this are easily captured using BART.

2.3 Priors

Our model involves different blocks of parameters or latent states (e.g., the VAR block, the factor loadings, and the BART factors). For each of these blocks, earlier work in the literature has proposed a range of different priors and any combination of these can be used with our factor-BART VAR. We make particular choices from this set of standard priors as noted below. The only departure from standard choices is the prior we use on Λ_f . In this case, we consider a row-wise shrinkage prior (see, e.g., [Huber and Feldkircher, 2019](#); [Kastner, 2019](#)). Particularly, we consider a Horseshoe prior ([Carvalho, Polson, and Scott, 2009](#)) that has row-specific global shrinkage parameters:

$$\lambda_{f,ij} \sim \mathcal{N}(0, \psi_{f,ij}^2 \tau_{f,i}^2), \quad \psi_{f,ij} \sim \mathcal{C}^+(0, 1), \quad \tau_{f,i} \sim \mathcal{C}^+(0, 1),$$

for $i = 1, \dots, M$ and $j = 1, \dots, Q_f$ and $\mathcal{C}^+(0, 1)$ denotes the half-Cauchy distribution. The row-wise scaling parameters $\tau_{f,i}$ shrink a particular row towards zero. Setting $\tau_{f,i} \approx 0$ would therefore imply that the resulting i^{th} equation is linear. The presence of the local shrinkage parameters $\psi_{f,ij}^2$ effectively allows for selecting a particular nonlinear form, if

warranted by the data.

We also use a Horseshoe prior on the VAR coefficients:

$$a_{ij} \sim \mathcal{N}(\underline{a}_{ij}, \psi_{a,ij}^2 \tau_a^2), \quad \psi_{a,ij} \sim \mathcal{C}^+(0, 1), \quad \tau_a \sim \mathcal{C}^+(0, 1).$$

Here, \underline{a}_{ij} is a prior mean that equals 0.8 if $i = j$ and 0 otherwise. Note that this prior hyperparameter choice is centered over coefficient values that imply that the elements of \mathbf{y}_t are each persistent AR processes. Hence the nonlinear factor part of the model has a strong tendency to soak up deviations from the persistent part of \mathbf{y}_t .

In contrast to the prior on the factor loadings, $\mathbf{\Lambda}_f$, the prior on the linear VAR part of the model features a single global shrinkage parameter and hence small values of τ_a force all elements in \mathbf{A} to zero. The idiosyncratic scaling parameters then allow for non-zero effects by leading to a heavy-tailed marginal (of $\psi_{a,ij}$) prior on a_{ij} .

On the elements of $\mathbf{\Lambda}_q$, $\lambda_{q,ij}$, we use Gaussian priors with zero mean and variance 10^2 . This noninformative choice implies little shrinkage on the elements of $\mathbf{\Lambda}_q$. In our structural analysis of Section 5 where we use sign restrictions, we modify this prior to be a truncated Gaussian distribution.

For the diagonal elements in $\mathbf{\Omega}$ and \mathbf{V}_q we consider conjugate inverse Gamma priors with hyperparameters a_ω , b_ω and a_q and b_q . In all our empirical work we set $a_\omega = b_\omega = 0.01$ and $a_q = 30$ and $b_q = 3$.

On the regression trees we use the standard prior setup proposed in [Chipman, George, and McCulloch \(2010\)](#). This prior involves three aspects. First, we need to specify the probability that a given node is non-terminal. This probability decreases in the depth of the node under consideration. Let d denote the current depth of some node then we set the probability that this node is non-terminal as $\mathbf{a}(1+d)^{-\mathbf{b}}$ with $\mathbf{a} = 0.95$ and $\mathbf{b} = 2$ being the standard hyperparameter choice of [Chipman, George, and McCulloch \(2010\)](#). Second, we need to specify a stochastic law for setting up the decision rules. Here, we assume that the splitting variable assignments are uniformly distributed so that, a priori, each splitting variable is equally likely. Third, and conditional on the chosen splitting variable, we use a uniform prior on the discrete set of splitting values of the

corresponding splitting variable.

On the terminal node parameters $\boldsymbol{\mu}_{i,s}$ we use a Gaussian prior. We follow [Chipman, George, and McCulloch \(2010\)](#) and normalize the responses (in our case the factors) to be between -0.5 and 0.5 . Then, for each element of $\boldsymbol{\mu}_{i,s}, \mu_{ij,s}$, our prior assumes:

$$\mu_{ij,s} \sim \mathcal{N}\left(0, \frac{0.5}{S\sqrt{\mathbf{m}}}\right).$$

Here, \mathbf{m} denotes a variance hyperparameter that we set equal to 2. This specification for the prior variance implies that for larger values of S , the prior variance declines and hence each tree is expected to explain less variation in the responses. This is consistent with the notion that each of the trees acts as a weak learner.

2.4 Posterior inference in the factor-BART VAR

Multiplying the priors discussed in the previous subsection with the likelihood derived in Sections 2.1 and 2.2 produces a joint posterior distribution that is unfortunately intractable. However, given that most priors are (conditionally) conjugate we can easily derive an MCMC algorithm — more specifically, a Gibbs sampler — which sequentially draws the parameters and latent quantities of the model in different blocks. Since all these blocks are standard, we provide only an outline of our MCMC methods here and relegate further details to the appendix.

The full conditional posterior distributions take the following forms:

- The VAR parameters, \mathbf{A} , are sampled equation-by-equation (conditional on \mathbf{q}_t and \mathbf{f}_t) from multivariate Gaussian posteriors using textbook linear Bayesian regression methods.
- The factor loadings, $\boldsymbol{\Lambda}_f$ and $\boldsymbol{\Lambda}_q$, are also simulated from multivariate Gaussian posteriors using textbook Bayesian methods for independent regression models with \mathbf{f}_t and \mathbf{q}_t acting as regressors.
- The factors \mathbf{f}_t of the model’s conditional mean are sampled conditional on $\mu(x_t)$ (and other model parameters) from Gaussian distributions.

- The factors \mathbf{q}_t of the model’s innovation term are sampled from Gaussian distributions as in a standard static factor model.
- $\mu_j(x)$ is, conditional on the $\{f_{jt}\}_{t=1}^T$ (the j^{th} element of \mathbf{f}_t), a standard BART regression model so that the methods outlined in [Chipman, George, and McCulloch \(2010\)](#) can be directly applied.
- The error and factor variances are all sampled from inverse Gamma distributions.
- The hyperparameters of the Horseshoe prior on \mathbf{A} and $\mathbf{\Lambda}_f$ are simulated using the algorithm proposed in [Makalic and Schmidt \(2015\)](#).

In principle, we could sample the trees marginally of the factors in \mathbf{f}_t to improve mixing of the trees. However, this leads to models with TM observations and evaluation of the likelihood becomes cumbersome. Hence, we opt for a conditional sampler. We find (in results omitted in the interest of brevity) our sampler to mix well.

There are several ways of selecting the numbers of factors Q_f and Q_q . For a structural application, it makes sense to set Q_q to the number of shocks the researcher wants to identify. In a forecasting application, standard forecast metrics (e.g., log predictive likelihoods), information criteria or marginal likelihoods can be used. However, we prefer to choose a fairly large number of factors and use a prior such as the Horseshoe on the columns of $\mathbf{\Lambda}_q$ and $\mathbf{\Lambda}_f$ and let it automatically remove unnecessary factors from the model by shrinking factor loadings to zero.

3 Artificial data exercises

3.1 Design of the Monte Carlo study

In this section, we carry out a small empirical exercise involving artificial data. The main contribution of our model lies in the BART treatment of the factors. Thus, we focus our study on the ability of BART to uncover various types of nonlinearity in the factors. Our data generating processes (DGPs) differ in the way the factors are generated.

We generate artificial data sets of $M = 16$ time series of length $T \in \{250, 500\}$. The choice of M is moderately large and typical of what is used in the VAR literature. The choices for T are the sort which often occur with quarterly and monthly macroeconomic data sets.

We use the following general DGP:

$$\mathbf{y}_t = \mathbf{A}_1 \mathbf{y}_{t-1} + \mathbf{\Lambda}_1 \mathbf{f}_t + \mathbf{\Lambda}_2 \mathbf{q}_t + \boldsymbol{\eta}_t, \quad \boldsymbol{\eta}_t \sim t_\nu(\mathbf{0}, 0.01^2 \times \mathbf{I}_{16}), \quad \mathbf{q}_t \sim \mathcal{N}(\mathbf{0}, \mathbf{I}_2), \quad \mathbf{y}_0 = \mathbf{0},$$

where \mathbf{A}_1 has $\text{diag}(\mathbf{A}) = 0.45$ and off-diagonal elements drawn from $\mathcal{N}(0, 0.01^2)$, the elements of $\mathbf{\Lambda}_1$ are drawn from $\mathcal{N}(0.35, 0.1^2)$, and the elements of $\mathbf{\Lambda}_2$ are drawn from standard Gaussian distributions. Note that we are assuming $Q_q = 2$ and are allowing $\boldsymbol{\eta}_t$ to be t -distributed which contrasts with the Gaussianity assumption made in (5). The t -distribution assumption allows us to investigate whether our nonlinear factor structure is also useful for modeling fat-tailed errors. In some of our DGPs, we set the degrees of freedom to $\nu = 4$ (which implies heavy-tailed errors) and in others we set $\nu = 10^4$ (which effectively implies Gaussianity).

In all cases, we consider factors that arise from a Gaussian distribution with different choices for the mean with covariance close to zero and set $Q_f = 3$:

$$\mathbf{f}_t \sim \mathcal{N}(\mu(\mathbf{y}_{t-1}), 10^{-4} \times \mathbf{I}_3).$$

We introduce four different laws of motion for the conditional means of the factors. Three of them assume that the mean of \mathbf{f}_t evolves according to nonlinear functions of lagged observables \mathbf{y}_{t-1} and heavy-tailed shocks (i.e., $\nu = 4$) whereas one assumes linearity by setting $\mathbf{\Lambda}_1 = \mathbf{0}$ and features effectively Gaussian shocks (i.e., $\nu = 10^4$). We refer to the linear DGP as DGP 1. DGP 2 is chosen as a highly nonlinear form not associated with any commonly used macroeconomic model. DGP 3 is a threshold specification which is commonly used in many papers. The final DGP, DGP 4, implies size and sign asymmetries.

The three nonlinear DGPs assume that the mean of the factors evolves according to:

DGP 2: $\mu(\mathbf{x}_t) = \mathbf{B}_1 \cos(\mathbf{y}_{t-1} \cdot y_{t-1,1} \cdot y_{t-1,3} \cdot \pi) + \mathbf{B}_2 |\mathbf{y}_{t-1} - 0.5| + \mathbf{B}_3 \sin(\mathbf{y}_{t-1})$. All operations inside trigonometric functions and the absolute value are element-wise. This DGP is inspired from the statistics literature (see, e.g., [Chipman, George, and McCulloch, 2010](#)). In terms of the properties of the simulated time series this DGP implies cyclical movements of \mathbf{f}_t with length and intensity of the waves being driven by the lagged endogenous series.

$$\text{DGP 3: } \mu(\mathbf{x}_t) = \begin{cases} \mathbf{B}_1 \mathbf{y}_{t-1} & \text{if } y_{1t-1} < 0 \\ \mathbf{B}_2 \mathbf{y}_{t-1} & \text{if } y_{1t-1} > 0. \end{cases}$$

This is a nonlinear process with endogenous regime switch, where the switching depends on the sign of the first component of \mathbf{y}_{t-1} . Similar processes have been considered in, e.g., [Kolesár and Plagborg-Møller \(2024\)](#).

$$\text{DGP 4: } \mu(\mathbf{x}_t) = \mathbf{B}_1 \mathbf{y}_{t-1}^3 + \mathbf{B}_2 \mathbf{r}_t,$$

where $\mathbf{y}_{t-1}^3 = \mathbf{y}_{t-1} \odot \mathbf{y}_{t-1} \odot \mathbf{y}_{t-1}$ is applied element-wise and the j^{th} element of \mathbf{r}_t is given by $r_{jt} = \max(0, y_{jt-1})$ for $j = 1, \dots, 16$. This DGP resembles the one studied in, e.g., [Gonçalves, et al. \(2024\)](#) and [Hauzenberger, et al. \(2025\)](#) and implies size and sign asymmetries in how \mathbf{y}_t reacts to changes in \mathbf{y}_{t-1} .

In both cases, the elements of the matrices \mathbf{B}_j in the DGPs are set at values sampled from Gaussian distributions with mean zero and variances for $\mathbf{B}_1, \mathbf{B}_2, \mathbf{B}_3$ equal to $0.15^2, 0.075^2$ and 0.1^2 , respectively.

From each DGP, we draw 50 realizations of time series of length T . For each of the 50 realizations, we estimate the model based on the first $T - h$ observations and compute out-of-sample predictive distributions at horizons $h = 1$ through $h = 8$. Predictive performance is assessed through log predictive likelihoods (LPLs) and continuous ranked probability scores (CRPSs). In each Monte Carlo data set, we compute these scores for each of the 16 variables and then take an average across variables in order to simplify reporting. Throughout the paper, the focus on density forecast performance provides a broader picture on potential accuracy gains from using our model.

In what follows, in estimates for each artificial data set we consider the factor-BART VAR with $Q_f \in \{3, 6, 12\}$ nonlinear factors while Q_q is set equal to 3 throughout (whereas

$Q_q = 2$ in the DGP). Each of the nonlinear models is then benchmarked to a linear VAR which is obtained by setting $Q_f = 0$ (while keeping $Q_q = 3$; in lieu of adding terminology to reflect the linear factor structure in the model’s innovation term, we simply refer to this as a VAR). Hence, accuracy differences reflect performance gains from adding nonlinear factors.

3.2 Monte Carlo findings

The results of our simulation exercise are depicted in [Table 1](#). The table shows the different values of T , DGP specifications, and number of BART factors Q_f in the rows. The columns include the forecast horizons per loss function (LPL and CRPS). All numbers are relative to the linear VAR benchmark (relative differences for LPLs and ratios for CRPSs).

Our main finding is that our factor-BART VAR forecasts better than the linear benchmark for all of the DGPs. For the nonlinear DGPs this is unsurprising, but also illustrates how BART methods can uncover a diverse range of nonlinear forms, including oscillatory, threshold, and asymmetric dynamics. The improvements are particularly marked at shorter forecast horizons for strongly nonlinear DGPs, where the flexibility of BART appears to translate most directly into more accurate predictive distributions.

What is more surprising is that it also forecasts slightly better than the linear model even when the DGP is linear. This effect is most pronounced for short samples and we conjecture that it reflects two mechanisms. First, BART-based regularization controls the predictive variance and mitigates possible small-sample bias in the estimates of the VAR coefficients. Second, BART, being nonparametric, can approximate near-linearity without leading to overfitting. As T increases, the benchmark model converges to the true linear DGP and regains its advantage, as can be seen from the reduced or reversed improvements for $T = 500$.

Another key finding is that factor-BART VAR forecasting performance is not sensitive to choice of the number of factors in the estimating model. Even though $Q_f = 3$ in the DGPs, setting Q_f to much larger values does not hurt forecast performance much.

			LPL			CRPS		
$Q_f \downarrow$			$h = 1$	$h = 4$	$h = 8$	$h = 1$	$h = 4$	$h = 8$
$T = 250$	DGP 1	3	0.31	0.32	0.32	0.83	0.81	0.81
		6	0.26	0.24	0.26	0.85	0.85	0.83
		12	0.18	0.17	0.17	0.87	0.88	0.87
	DGP 2	3	0.20	0.24	0.24	0.87	0.83	0.83
		6	0.14	0.16	0.17	0.90	0.88	0.87
		12	0.06	0.06	0.08	0.96	0.96	0.94
	DGP 3	3	0.21	0.25	0.24	0.87	0.83	0.85
		6	0.16	0.19	0.20	0.89	0.88	0.87
		12	0.05	0.05	0.06	0.97	0.97	0.97
DGP 4	3	0.09	0.06	0.03	0.95	0.95	0.96	
	6	0.06	0.06	0.01	0.93	0.96	0.95	
	12	0.03	0.01	-0.01	0.96	0.97	0.99	
$T = 500$	DGP 1	3	0.11	0.12	0.12	0.95	0.93	0.94
		6	0.17	0.18	0.16	0.93	0.91	0.92
		12	0.25	0.19	0.22	0.85	0.88	0.87
	DGP 2	3	0.31	0.29	0.27	0.81	0.82	0.83
		6	0.32	0.34	0.33	0.81	0.79	0.80
		12	0.27	0.24	0.24	0.82	0.85	0.85
	DGP 3	3	0.31	0.29	0.28	0.81	0.82	0.83
		6	0.31	0.31	0.28	0.82	0.81	0.83
		12	0.24	0.26	0.24	0.85	0.84	0.84
DGP 4	3	0.10	0.02	0.01	0.91	1.01	1.07	
	6	0.28	0.24	0.19	0.81	0.85	0.91	
	12	0.20	0.13	0.13	0.83	0.92	0.92	

Notes: The table shows average log score differences and CRPS ratios across 50 replications from each of the DGPs to the linear VAR (which sets $Q_f = 0$). Numbers greater than zero (lower than one) imply a better performance in terms of LPLs (CRPSs).

Table 1: Forecast performance based on synthetic data for 50 replications from the DGP.

This illustrates how our shrinkage prior is ensuring parsimony and removing the effect of extraneous factors in the estimating model.

The results are also robust to non-Gaussian innovation distributions. We find that the factor-BART VAR forecasts best when the DGP features heavy-tailed t_4 shocks, which are common in empirical macroeconomic and financial data. The improvement in CRPSs in such settings suggests that the model’s density forecasts remain well-calibrated under distributional mis-specification.

Finally, differences in LPL and CRPS patterns across horizons give us some information on the relationship between overall calibration and tail behavior of the models

since LPLs reward sharper tail fit, while CRPSs also penalize overconfident forecasts (see, e.g., Gebetsberger, et al., 2018; Waghmare and Ziegel, 2025). The occasional divergence between the two metrics reflects cases where our factor-BART VAR gains in sharpness do not always translate into uniformly better calibration, particularly at longer horizons in the linear DGP.

4 Application: Forecasting the US economy

The Monte Carlo simulations in the previous section show that if the DGP is nonlinear, our model has the potential to produce substantial gains in terms of density forecasting performance. In this section’s application, we consider whether this holds in a large US macroeconomic dataset, to which we apply our models to obtain forecasts of a range of variables.

4.1 Data, design of the forecasting exercise and model specification

In our applications, we take quarterly data from the FRED-QD database developed in McCracken and Ng (2021) and maintained at the Federal Reserve Bank of St. Louis. In particular, we use $M = 35$ major macroeconomic and financial time series from the database. As detailed in the variable list provided in Table A.1 of the appendix, the selected series include growth of real GDP and many of its main components, various measures of aggregate inflation, other indicators of the labor market and economic activity such as payroll employment and industrial production, the federal funds rate and various other interest rates covering longer maturities. Our set of selected variables is very similar to that used in the large Bayesian VAR of Crump, et al. (2025). We transform all variables to be stationary following recommendations from McCracken and Ng (2021), see Appendix Table A.1 for details. With transformations implemented, our data sample runs from 1976:Q3 to 2023:Q4.

The forecast design is as follows. We start with an initial estimation sample that ends

in 2001:Q4. After estimating the model we iteratively compute predictive distributions from $h = 1$ up to $h = 8$ -quarters-ahead. We then add one additional observation to the model estimation sample (i.e., use a recursive scheme) and repeat this procedure until we reach the end of the sample. Finally, after obtaining the predictive distributions for all observations in the holdout, we compute LPLs and CRPSs.

We consider models that set $p = 2$ and $Q_q = 3$ and focus on different values of $Q_f \in \{3, 6, 12\}$. The benchmark is a linear VAR that sets $Q_f = 0$ (while keeping $Q_q = 3$, i.e., keeping a linear factor structure in the model’s innovation term).

4.2 Predictive evidence

In this forecasting application, we focus on the accuracy of predictions for a few major measures of economic activity (GDP growth, industrial production growth, and the unemployment rate), several different measures of aggregate inflation (for the GDP price index, core and headline CPI inflation, and core and headline PCE inflation), as well as an interest rate (the 2-year Treasury yield). Table 2 reports relative LPLs and CRPSs for our factor-BART VAR compared to the linear VAR baseline (LPL entries greater than 0 and CRPS ratios lower than 1 mean our model is more accurate for the indicated variable and horizon). These results include forecasts through 2023:Q4; the appendix includes a corresponding table for forecasts through 2019:Q4, for which results are very similar.

These results show that, for measures of economic activity, the additional flexibility of our proposed model does not improve forecast accuracy relative to the linear baseline. There are some instances (i.e., for some variables at some horizons) of forecast gains, but in most cases, our model is either similar in accuracy or modestly less accurate than the baseline. For example, with $Q_f = 3$, the CRPS ratio is 1.02 for GDP growth at all horizons, and the CRPS ratio ranges from 0.99 to 1.01 across horizons for the unemployment rate. The same characterization applies to forecasts of the 2-year Treasury yield.

The flexibility of our proposed model yields larger, more consistent gains in the accuracy of inflation forecasts. The improvements in accuracy are comparable across the

	$Q_f \downarrow$	(a) LPL			(b) CRPS		
		$h =$			$h =$		
		1	4	8	1	4	8
Output and Labor Markets							
GDPC1	3	0.12	-0.01	-0.01	1.02	1.02	1.02
	6	0.01	-0.05	-0.04	1.07	1.05	1.05
	12	0.14	-0.06	-0.01	1.04	1.03	1.02
INDPRO	3	-0.34	-0.01	-0.00	1.01	1.01	1.01
	6	0.02	-0.04	-0.02	1.05	1.02	1.02
	12	0.15	-0.00	0.02	1.01	1.00	0.98
UNRATE	3	0.17	0.35	-1.68	0.99	0.99	1.01
	6	0.16	1.65	-0.82	1.09	1.05	1.04
	12	0.31	-0.18	1.79	1.06	1.03	1.02
Prices							
GDPCTPI	3	0.03	0.02	0.03	0.99	0.99	0.98
	6	0.18	0.18	0.16	0.91	0.91	0.92
	12	0.14	0.10	0.09	0.93	0.95	0.95
PCECTPI	3	0.05	0.04	0.04	0.98	0.98	0.97
	6	0.30	0.29	0.29	0.82	0.82	0.82
	12	0.21	0.15	0.19	0.87	0.90	0.88
PCEPILFE	3	0.03	0.02	0.02	0.98	0.99	0.99
	6	0.17	0.14	0.16	0.90	0.91	0.90
	12	0.12	0.07	0.08	0.93	0.95	0.95
CPIAUCSL	3	0.04	0.04	0.03	0.98	0.98	0.98
	6	0.23	0.25	0.26	0.87	0.84	0.83
	12	0.17	0.14	0.18	0.89	0.91	0.88
CPILFESL	3	-0.00	0.01	0.02	1.00	0.99	0.99
	6	-0.07	0.08	0.12	1.04	0.93	0.90
	12	-0.06	0.07	0.12	1.03	0.93	0.90
Interest rates							
GS2	3	0.03	0.02	0.02	0.98	0.99	0.99
	6	-0.05	-0.04	-0.05	1.05	1.05	1.04
	12	-0.08	-0.09	-0.08	1.08	1.08	1.07
Joint log predictive likelihood							
	3	-0.38	0.00	-0.63			
	6	0.77	0.37	0.98			
	12	1.67	1.25	1.11			

Notes: The table shows forecast losses relative to the VAR. Panel (a) shows the differences in log predictive likelihood while panel (b) shows the continuous ranked probability score. Joint refers to the joint predictive likelihood over the full set of the focus variables we consider in this table.

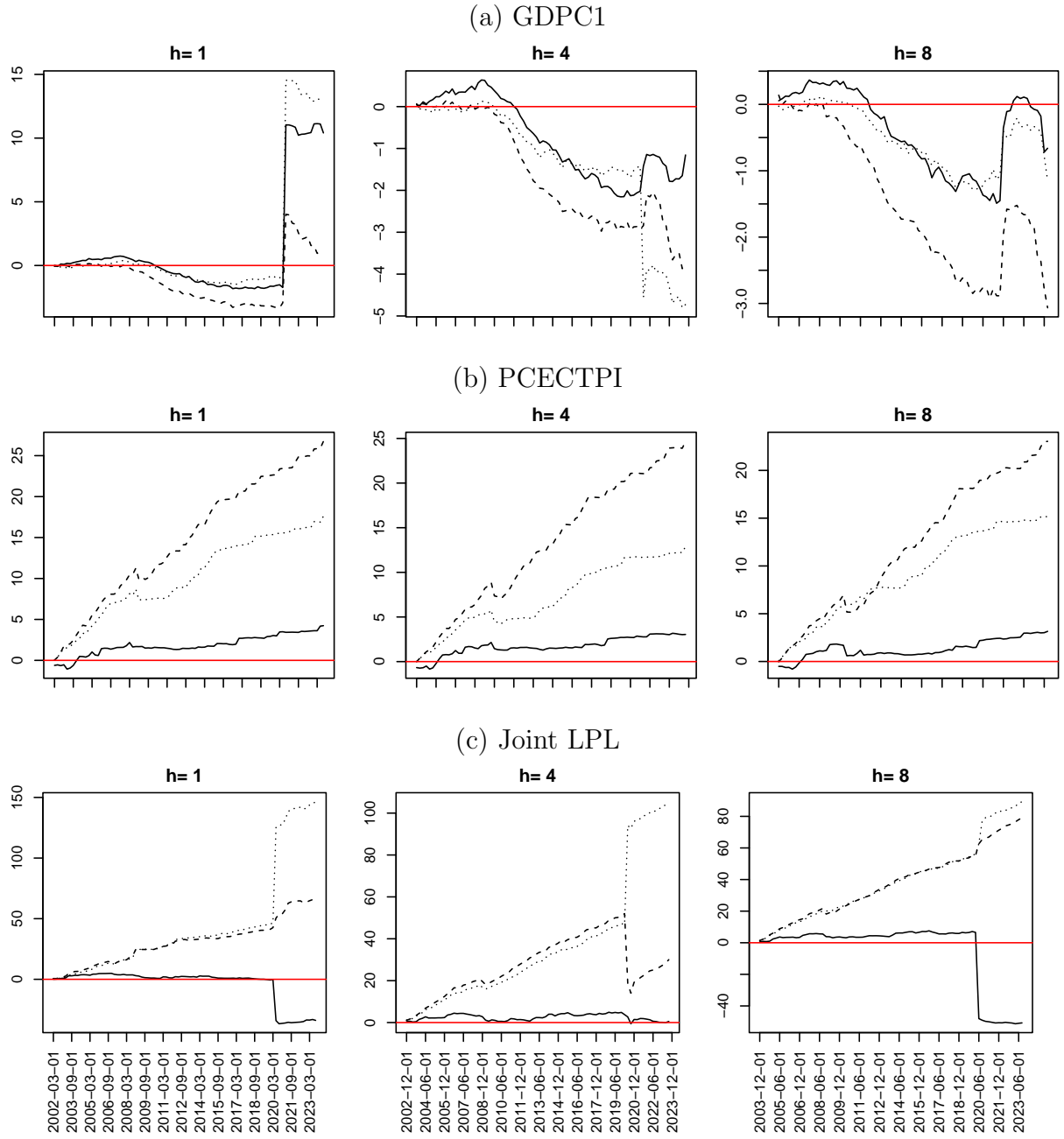
Table 2: Average log predictive likelihoods and continuous ranked probability scores to the VAR

horizons of $h = 1, 4$, and 8 quarters. With the number of factors set to $Q_f = 3$, the gains in density forecast accuracy are consistent but small, usually between 1 and 3 percent in CRPS and between 2 and 5 percent in LPL. Bigger gains are achieved with more factors

in the model. With $Q_f = 6$, the gains in accuracy are roughly 10 percent for CRPS and 20 percent for LPL. Performance is very similar across the headline CPI and PCE measures of headline inflation (CPIAUCSL and PCECTPI). The same applies to the core CPI and PCE measures (CPILFESL and PCEPILFE). Consistent with other work in the inflation forecasting literature, our model achieves larger gains in forecast accuracy for the headline inflation measures than for the core inflation measures.

The bottom panel of the table provides joint log predictive likelihood results for the set of economic activity, inflation, and interest rate variables indicated in the preceding rows of the table. These joint scores confirm that our proposed flexible, nonlinear model can yield sizable gains in density forecast accuracy. By this joint measure, our factor-BART VAR is about as accurate as a linear VAR with a small number of nonlinear factors ($Q_f = 3$) but substantially more accurate than the benchmark with larger numbers of factors included ($Q_f \in \{6, 12\}$).

To assess the performance of our models in density forecasting over time, Figure 1 reports cumulative LPLs over the forecast evaluation sample. In the interest of brevity and chart readability, the figure provides results for selected illustrative variables — GDP growth and headline PCE inflation — and the joint LPLs. In the case of GDP growth (panel a), the cumulative LPL shows little change in the several years before the Great Recession and then steadily declines for most of the sample, with the linear VAR yielding modestly better forecasts than our nonlinear factor specification. At some horizons, the nonlinear specification briefly improves in relative terms around the time of the COVID pandemic’s outbreak in 2020. In the case of PCE inflation, the steady gains in LPLs over time shown in panel b of Figure 1 indicate that our nonlinear model consistently improves forecast accuracy consistently over the sample, more so with the larger number of factors than with $Q_f = 3$ (consistent with the full-sample results discussed above).



Notes: The figures show the evolution of the cumulative log predictive likelihood of the corresponding nonlinear VAR to the linear benchmark VAR.

Legend: — is the model with $Q_f = 3$, -- the one with $Q_f = 6$, and ... refers to the one with $Q_f = 12$ factors.

Figure 1: Log predictive likelihoods relative to the VAR

5 Structural analysis using a small nonlinear model of the US economy

Having established some benefits of our proposed model for out-of-sample forecasting, this section’s application shows its ability to capture nonlinearities in responses to structural shocks. In this application, we estimate a smaller model with $M = 9$ series. As listed in the rows of [Table 3](#), these variables include growth of GDP, consumption, fixed investment, and hourly labor compensation, the unemployment rate, core PCE inflation, consumer sentiment, and the federal funds rate (using the transformations of [McCracken and Ng \(2021\)](#)). The model also includes the excess bond premium (EBP) of [Gilchrist and Zakrajšek \(2012\)](#) (using the current, updated series available from [Favara, et al., 2016](#)). In view of the moderate variable count, we set the number of common nonlinear factors to $Q_f = 2$. We use sign restrictions as in studies such as [Korobilis \(2022\)](#) to identify shocks to demand, supply, monetary policy, and financial conditions. Accordingly, we set the number of common shocks to $Q_q = 4$.

The first subsection below starts with some reduced-form results on the estimated loadings Λ_f , it shows how the factors and observed variables vary nonlinearly with the covariates and discusses the estimated nonlinear factors. The second subsection provides further information on how we identify the structural shocks and presents the impulse response functions for a monetary policy shock.

5.1 Reduced-form results

[Figure 2](#) provides in a heatmap (larger positive in green, more negative in red) the posterior median estimates of the loadings for each variable on the two common factors (i.e., elements of Λ_f). The loadings capture the contemporaneous relationships between the factors and the endogenous variables and, thus, these loadings can be seen as measures of the static relationships. The estimated loadings suggest the first factor is linked to a measure of economic activity, with relatively positive loadings on GDP growth and consumption growth and a relatively negative loading on the unemployment rate. The

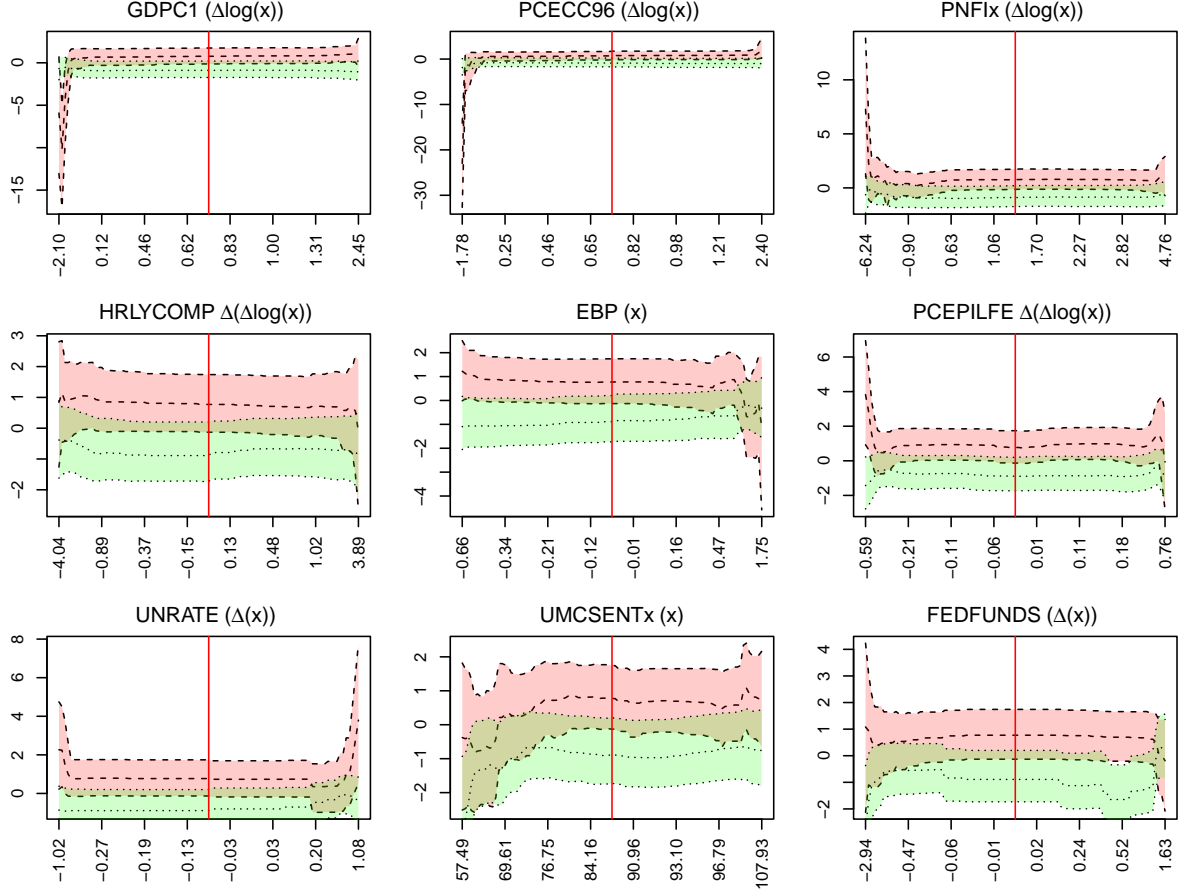
1	0.14	0.15	0.08	-0.05	-0.01	0.05	-0.19	0.02	0.01
2	-0.06	-0.02	-0.07	-0.00	0.01	-0.04	0.04	0.00	-0.51
	GDPG1	PCECC96	PNFIX	HRLYCOMP	EBP	PCEPILFE	UNRATE	UMCSENTx	FEDFUNDS

Figure 2: Heatmap of the posterior median of Λ_f

second factor appears to be linked to monetary policy, with a loading of -0.51 on the federal funds rate and correspondingly small negative loadings on GDP and its components and a positive loading.

To shed more light on the nonlinear factor functions, [Figure 3](#) shows the posterior distributions of how the functions $\mu_1(\mathbf{x}_t)$ and $\mu_2(\mathbf{x}_t)$ change with movements in \mathbf{x}_t . This is done by setting the elements in \mathbf{x}_t that correspond to a particular variable to different quantiles. These quantiles are defined on a fine grid that starts at the one percent quantile and ends with the 99 percent quantile in 1 percent increments. We keep all other elements in \mathbf{x}_t at their sample means so that these quantities measure the reaction of the latent factors to changes in selected covariates while everything else is unchanged at relatively normal levels. While the factor loadings reported above capture static relationships, these posterior distributions of how the functions change can be seen as capturing dynamic relationships between the factors and endogenous variables, including the co-movement that occurs at lags.

As indicated in the top left panel of [Figure 3](#), across most values of GDP and consumption growth, the first factor displays little variation. However, left-tail readings of GDP and consumption growth (akin to those observed in recessions) are each associated with sharp, nonlinear drops in the first factor. The first factor also displays no reaction to changes in the unemployment rate across most of the distribution of unemployment, except in both tails; large changes in unemployment in either direction are associated with significant increases in the first factor. Despite the small loading of the first factor on the excess bond premium, very high values of the bond premium are associated with large



Notes: The figure shows how the factors change with the explanatory variables in \mathbf{x}_t . Red areas correspond to the dynamics of the first factor whereas green areas correspond to the dynamics of the second factor. Lines (both dashed and dotted) refer to the corresponding 16th, 50th and 84th percentiles of the posterior distribution.

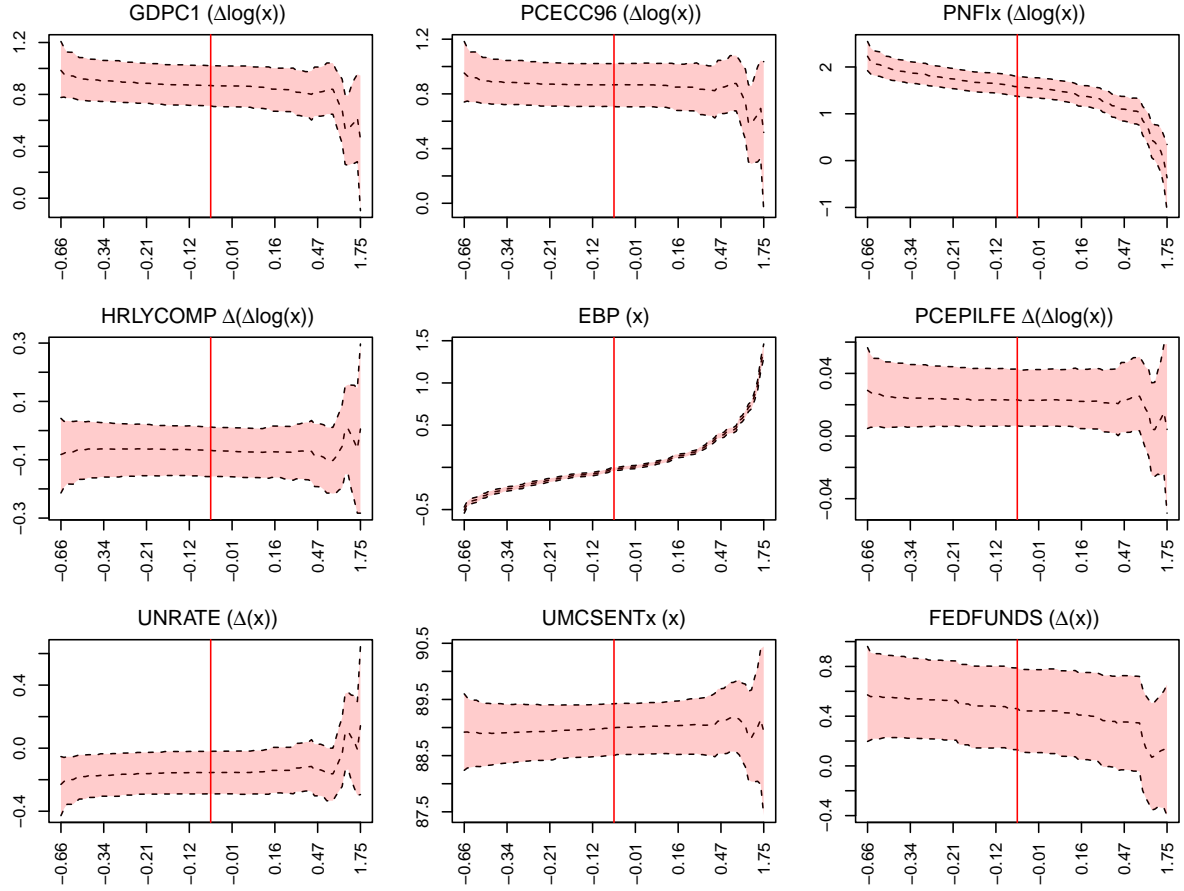
Figure 3: Sensitivity of the factors to changes in \mathbf{x}_t

declines in the first factor that evidently occur with lags and not just contemporaneously.

Similarly, the second factor also appears to evolve linearly with most variables over most of their marginal distributions, but with some noticeable exceptions that occur in tails. For example, low values of consumer sentiment are associated with sizable declines in the second factor. The second factor also appears to show discrete shifts that occur across broad ranges of values for changes in the federal funds rate, but rises more significantly with big increases in the funds rate.

In sum, our results indicate that for most variables, there is some evidence that nonlinearities exclusively arise in the tails. This is because both factors only exhibit appreciable tail variation with respect to changing the variables. When taking normal values (defined as intermediate values between the 1 and 99 percent quantiles), most factors are constant and hence the conditional mean is mostly determined by the VAR

part of the model.



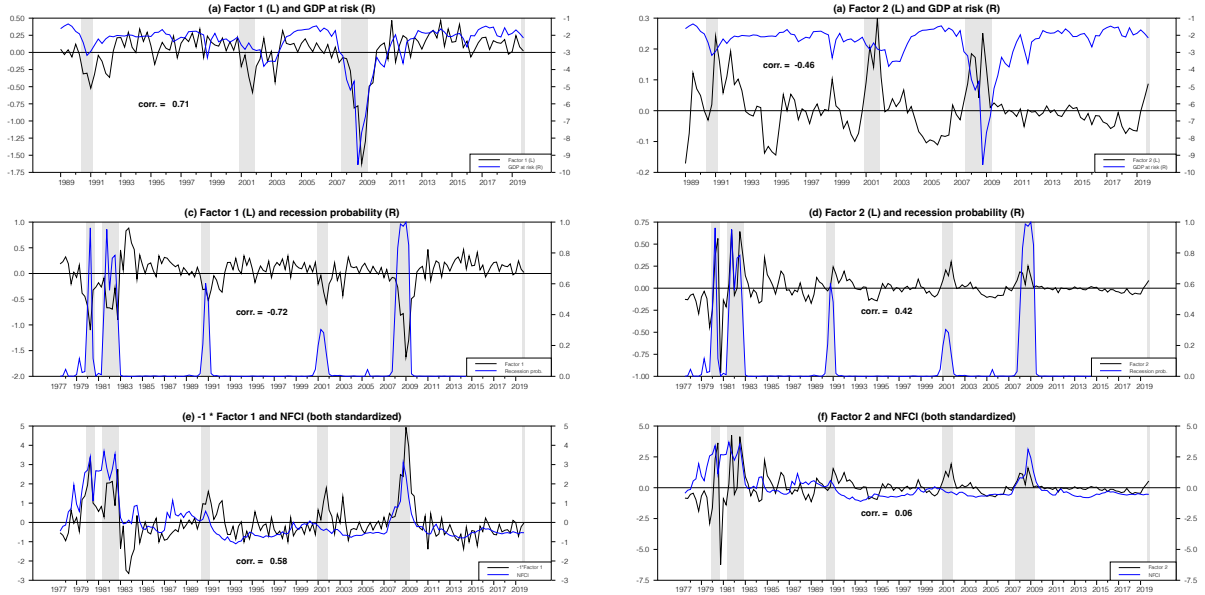
Notes: The figure shows how the observed series change with the EBP. Red areas and lines (both dashed and dotted) refer to the 16th, 50th and 84th percentiles of the posterior distribution.

Figure 4: Sensitivity of the observed series to changes in the EBP

To shed some light on the role of financial conditions in macroeconomic developments, Figure 4 shows posterior distributions of how the variables of the model change with movements in the lagged EBP. Movements in the EBP impact other variables through both the linear VAR component and the nonlinear functions $\mu_1(\mathbf{x}_t)$ and $\mu_2(\mathbf{x}_t)$ (multiplied by $\mathbf{\Lambda}_f$).

Here, too, relationships of other variables to the EBP seem largely linear across much of the distribution, but show nonlinearities with high values of the bond premium. The linear relationship detected for values below the 95 percent quantile of the EBP differ in strength, being somewhat stronger for investment growth and the EBP itself while being much more muted for the other series (or even non-existent). When bond premia become large, they are associated with strongly reduced growth of GDP and consumption and

increases in the unemployment rate, as well as some reduction in the federal funds rate.



Notes: The figure shows the evolution of the nonlinear factors 1 and 2 (in black) compared to various indicators of business cycle risk and recessions (in blue). These are the NY Fed's estimates of GDP at risk (panels a-b), Chauvet-Piger estimates of recession probabilities (panels c-d), and the Chicago Fed's NFCI (panels e-f), and their correlations.

Figure 5: Evolution of the nonlinear factors f_t alongside measures of business cycle risk and recessions

To provide another window into the capability of our model's factors to capture tail dynamics, Figure 5 reports time series of the posterior means of factors 1 and 2 with several existing measures of business cycle risk and recessions.⁴ In the interest of chart readability, the figure ends the sample in 2019Q4 to avoid the extreme volatility induced by the outbreak of the COVID-19 pandemic.

Panels (a) and (b) show that our estimates of nonlinear factors are connected to left-tail risks of GDP growth as captured by the Federal Reserve Bank of New York's published estimates of GDP growth at risk, measured as the 10 percentile of the conditional distribution of four quarter-ahead average GDP growth. In particular, our first factor has a strong resemblance to GDP at risk, with a correlation of 0.71 in quarterly

⁴We obtained the GDP at risk estimates from the website of the New York Fed and formed quarterly time series as within-quarter averages of the underlying monthly estimates. We obtained the recession probabilities from FRED (mnemonic RECPROUSM156N) and formed quarterly time series as within-quarter averages of the underlying monthly estimates. We also obtained the quarterly NFCI (averaging weekly data) from FRED (mnemonic NFCI).

data for 1989-2019. Our second factor is also connected to growth at risk, but not as strongly, with a correlation of -0.49.⁵ Panels (c) and (d) indicate that our factors are very similarly correlated with estimates of the probability of the economy being in a recession produced by a dynamic-factor Markov-switching model applied to a few major macro time series, which has been shown to be effective for its intended purpose in [Chauvet and Piger \(2008\)](#).

In view of the emphasis that the growth at risk literature has placed on the connection of business cycle risk to financial conditions as measured with indices like the Federal Reserve Bank of Chicago’s NFCI (e.g., [Adrian, Boyarchenko, and Giannone, 2019](#)), panels (e) and (f) compare our factor estimates to the NFCI. (Recall that the NFCI is not one of the variables in the model.) To facilitate comparisons, these panels report the factors and NFCI in standardized terms (i.e., transformed to mean 0 and variance 1), and we flip the sign of factor 1. With the sign change, factor 1 has a significant connection to financial conditions as measured by the NFCI, with a correlation of -0.58, whereas factor 2 has little connection to this particular measure of financial conditions, with a correlation of 0.06.

Together, these simple comparisons show that, while our model is quite different from the quantile regression underlying the New York Fed’s growth at risk estimate or a Markov switching model used for recession detection, it has the flexibility to capture tail dynamics in a similar fashion. It also has the flexibility to reflect fluctuations in a variable like the NFCI commonly linked to business cycle risk and downturns.

5.2 Nonlinear responses to identified monetary policy shocks

Turning to impulse response estimates for monetary policy shocks, as noted above we use sign restrictions to identify shocks to demand, supply, monetary policy, and a financial shock. Sign restrictions are implemented in the tradition of [Baumeister and Hamilton \(2015\)](#) and [Korobilis \(2022\)](#) through priors truncated to the respective set implied by the

⁵Over a longer 1977-2019 sample of factor estimates, the correlation between the posterior means of factors 1 and 2 is -0.26.

sign restrictions. In our framework, this implies changing the Gaussian prior on $\mathbf{\Lambda}_q$ to a truncated Gaussian prior to attach an economic meaning to the elements in \mathbf{q}_t (and thus avoid identification issues related to column switching). We achieve this by setting:

$$\lambda_{q,ij} \sim \begin{cases} \mathcal{N}_{0,\infty}(0, 10^2), & \text{if shock } j \text{ is restricted to have a positive impact effect on variable } i, \\ \mathcal{N}_{-\infty,0}(0, 10^2), & \text{if shock } j \text{ is restricted to have a negative impact effect on variable } i, \\ d_c(\lambda_{q,ij}), & \text{if shock } j \text{ is restricted to have a fixed impact effect } c \text{ on variable } i, \\ \mathcal{N}(0, 10^2), & \text{if shock } j \text{ exerts an unrestricted impact effect on variable } i. \end{cases}$$

Here, we let $d_c(\lambda_{ij})$ denote the Dirac delta function which puts point mass on c . If we use a truncated prior the posterior simulation step for $\mathbf{\Lambda}_q$ changes slightly. Instead of simulating the rows of $\mathbf{\Lambda}_q$ from unrestricted Gaussian distributions, the truncated prior implies that the posterior is truncated to the set implied by the prior.

Table 3 lists the sign restrictions. For example, following typical practice, a one standard deviation monetary policy shock (tightening) is identified as a shock that raises the federal funds rate by $c = 25$ basis points and reduces GDP growth, increases the unemployment rate, and reduces core PCE inflation. A shock to financial conditions is identified as a shock that raises the EBP by 1 unit and reduces GDP growth, consumption, investment, consumer sentiment, and core PCE inflation, and raises the unemployment rate, leading to a reduction of the federal funds rate. These identifying restrictions are similar to those used in studies such as [Chan, Matthes, and Yu \(2025\)](#).

In the interest of brevity, we focus on shocks to monetary policy. To assess possible nonlinearities, we consider the impacts of shocks differing in sign and size. Specifically, we estimate impulse response functions (IRFs) to positive and negative shocks to monetary policy, with the responses to the negative shock multiplied by -1 to facilitate comparing responses to positive and negative shocks. One set of results uses a shock size δ of 1 standard deviation, and a second set of results uses shock size of 3 standard deviations in order to check possible differences with large shocks. In all cases, we compute the impulse response functions (IRFs) using the generalized IRF approach of [Koop, Pesaran, and Potter \(1996\)](#).

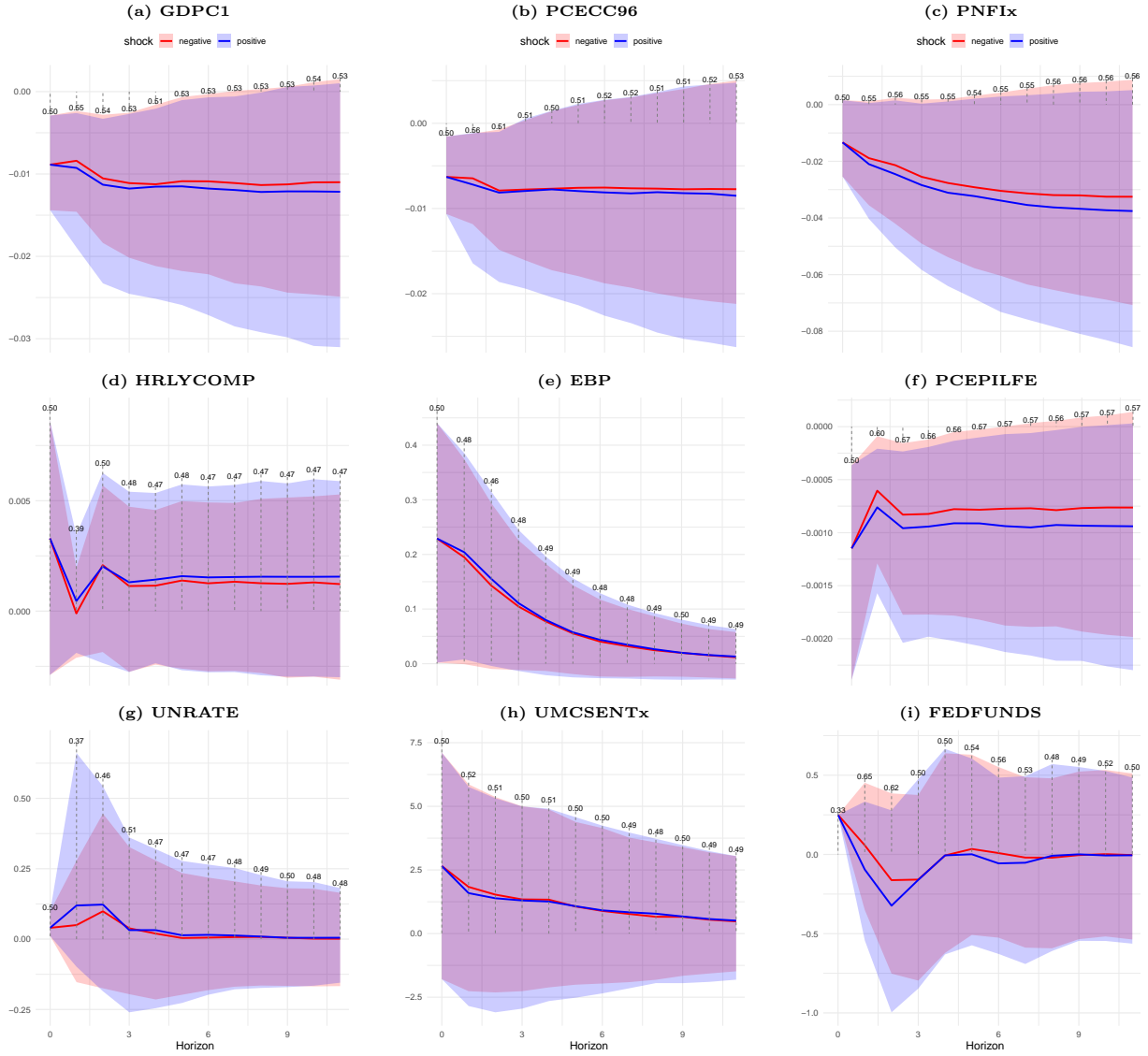
Variable	Demand	Monetary	Supply	Financial
GDPC1	+	—	—	—
PCECC96			—	—
PNFI _x	—			—
HRLYCOMP				
EBP				c
PCEPILFE	+	—	+	—
UNRATE	—	+	+	+
UMCSENT _x	+			—
FEDFUNDS	+	c		—

Notes: '+' refers to a positive impact reaction, '-' to a negative one, 'c' implies that we fix the impact effect whereas no sign means that we have introduced no restriction.

Table 3: Sign restrictions used to identify the structural factors in the model

Starting with the case of the small (1 standard deviation) shock to the federal funds rate, Figure 6 reports the posterior median responses for positive and negative shocks, along with 68 percent credible sets. With a small shock, there appears to be little asymmetry in responses to tightenings versus easings of monetary policy; results are quite similar in absolute value. A policy tightening tends to slow economic activity (e.g., reducing GDP growth and raising unemployment) and inflation, whereas an easing has the reverse impacts. To gauge posterior evidence of differences in responses for positive versus negative shocks to the funds rate, each panel provides for each horizon of impact the posterior probability that the reactions to a positive shock are stronger than the median reactions to a negative shock. (This measure is similar to the approach adopted by [Barnichon and Matthes \(2018\)](#) to assess the significance of asymmetries in IRFs.) In most cases, these posterior probabilities are around 50 percent, indicating similarity in the responses for positive and negative policy shocks, given a small shock size.

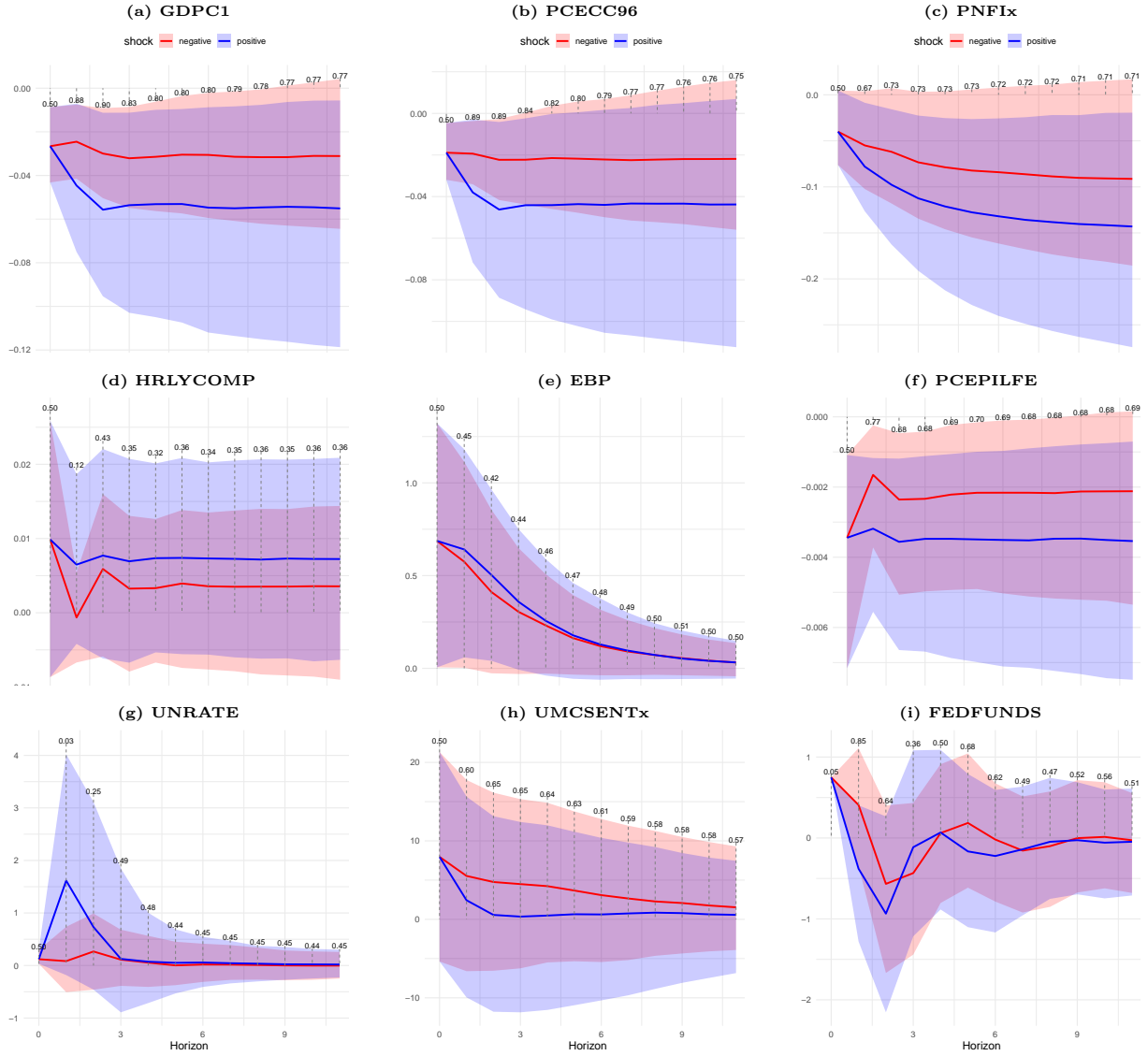
Turning to the case of a large (3 standard deviations) shock to the federal funds rate, Figure 7 reports the posterior median responses, along with 68 percent credible sets. A large shock yields more evidence of asymmetries in responses to tightenings versus easings of monetary policy. With a large shock, a significant tightening of monetary policy has bigger impacts on economic activity and inflation than does a corresponding easing of policy. For example, roughly four quarters following the shock, the impact on GDP growth (as well as consumption and investment) is roughly double (in absolute value) for



Notes: The figure shows the 16th and 84th posterior percentiles and median impulse responses to positive (contractionary) and negative (expansionary) monetary policy shocks. To facilitate comparability we multiply the IRFs to negative shocks by -1 . The numbers on top of the IRFs correspond to the posterior probability that the reactions to a positive shock are stronger than the median reactions to a negative shock.

Figure 6: Impulse responses to positive and negative 1 standard deviation monetary policy shocks

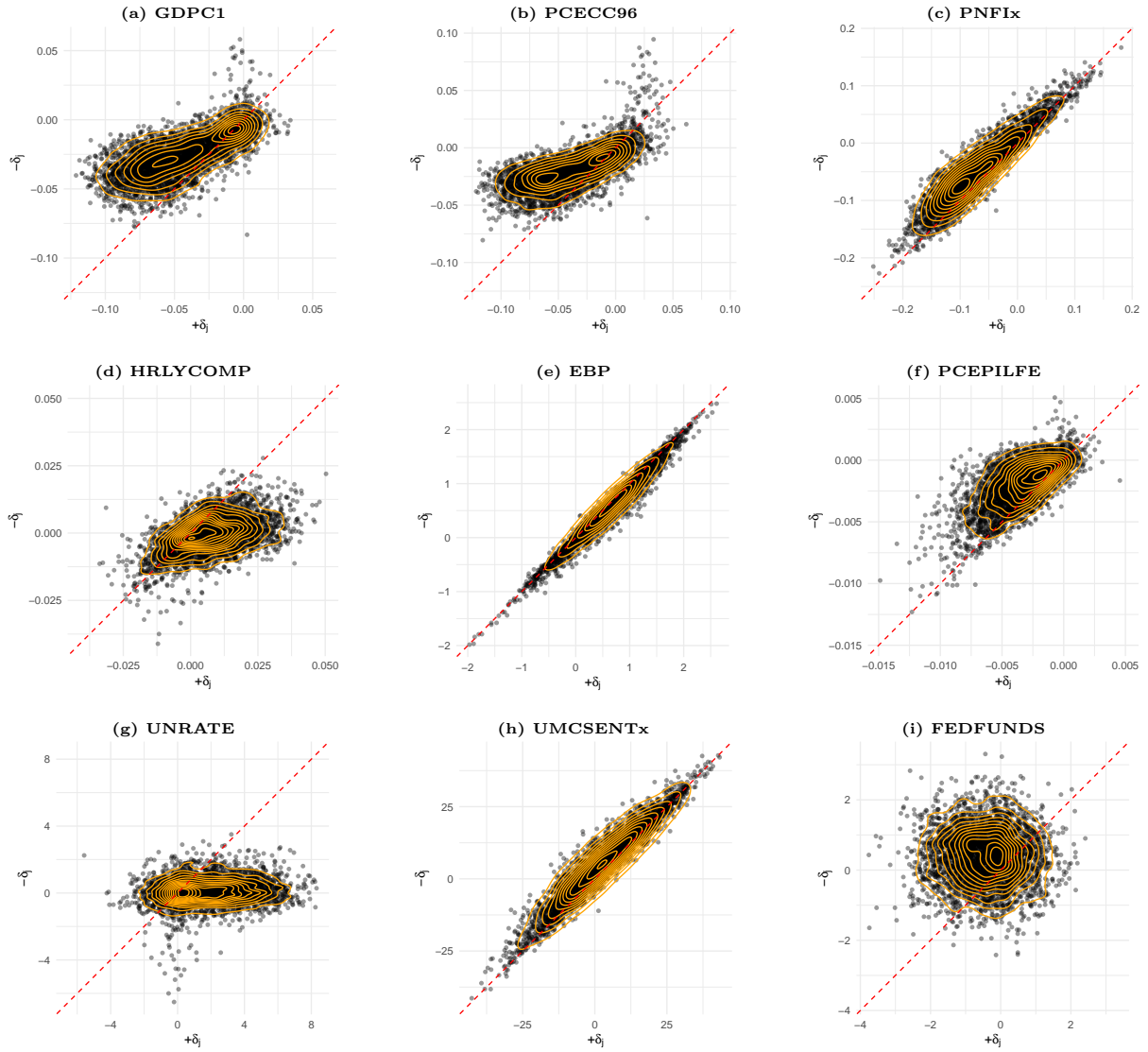
the tightening of policy as compared to the easing of policy. The posterior probabilities that the reactions to a positive shock are stronger than the median reactions to a negative shock indicate that the statistical evidence of differences is solid: For most measures of economic activity and for inflation, the posterior probabilities are usually between 75 and 80 percent. By comparison, the responses of the federal funds rate following the initial shock are comparable, with posterior probabilities of roughly 50 percent, such that the different responses of other variables to shocks of different signs do not appear to be driven by different paths of the funds rate.



Notes: The figure shows the 16th and 84th posterior percentiles and median impulse responses to positive (contractionary) and negative (expansionary) monetary policy shocks. To facilitate comparability we multiply the IRFs to negative shocks by -1 . The numbers on top of the IRFs correspond to the posterior probability that the reactions to a positive shock are stronger than the median reactions to a negative shock.

Figure 7: Impulse responses to positive and negative 3 standard deviation monetary policy shocks

To shed further light on the differences in posterior distributions for shocks of opposite sign, for the 1-quarter-ahead horizon (while not reported in the interest of brevity, results are qualitatively similar at horizons of 2 and 4 quarters) Figure 8 provides scatter- and contour plots (based on a kernel density smoother) to positive (contractionary, on the horizontal axis) and negative (expansionary, on the vertical axis) monetary policy shocks in the three standard deviation case. If the distributions for positive and negative shocks were the same, the dots and contours would be scattered along the diagonal line. For most variables, the contours are consistent with noticeably different posterior distribu-



Notes: The figure shows the one-quarter-ahead scatter- and contour plots (based on a kernel density smoother) of responses to positive (contractionary) and negative (expansionary) monetary policy shocks.

Figure 8: Scatterplots of one-quarter-ahead responses to positive and negative **three** standard deviation monetary policy shocks

tions of responses for positive and negative shocks. For example, in the case of GDP and consumption growth, relative to the diagonal line the contours are rotated up and to the right, reflecting larger impacts on growth from a funds rate increase than a corresponding large funds rate decrease. For the unemployment rate, relative to the diagonal line the contours are shifted well to the right, reflect bigger impacts on unemployment from a funds rate increase than a corresponding funds rate reduction.

Our findings of significant asymmetries in the responses to monetary policy shocks align with other evidence in the literature, obtained with different methods, such as [Angrist, Jorda, and Kuersteiner \(2018\)](#) and [Barnichon and Matthes \(2018\)](#). Within the semi-

parametric family of approaches, [Angrist, Jorda, and Kuersteiner \(2018\)](#) use a propensity score weighting estimator based on a “selection-on-observables identification condition in a potential outcomes framework.” Their estimates imply that the impacts of policy differ even with small policy shocks (of opposite sign). [Barnichon and Matthes \(2018\)](#) instead use a functional approximation of impulse responses that amount to local projection estimators with shape restrictions on the response functions. Their estimates also imply that the impacts of policy differ with the sign of the shock, treated as large in either case. While the approaches of these two papers focus on just the sign of the shock, one advantage of our model is that we are able to consider differences in responses that may arise due to both shock size and shock sign. For the policy shock, we find asymmetries in responses for the large shock but not the small shock.

6 Concluding remarks

We have proposed an extension to the standard VAR where departures from linearity are modeled using a nonlinear factor structure. The nonlinear factor is modeled using Bayesian regression tree methods. The use of a factor structure ensures parsimony and is motivated by the empirical findings that macroeconomic time series are typically found to be driven by a small number of factors. The fact that these factors are nonlinear and estimated nonparametrically reduces the risk of mis-specification. These features are of particular use for the researcher who expects their data set to exhibit nonlinearities but has little guidance as to the precise form these nonlinearities will take. In an artificial data exercise and an empirical study involving US macroeconomic data, we demonstrate the effectiveness of our methods and their ability to pick out patterns in the data that cannot be found using linear methods.

It would be straightforward to extend our model to allow for other features of the VAR to be modeled more flexibly. For instance, the assumption of Gaussian errors could be easily relaxed through a mixture of Gaussians. Or the error variances could be allowed to be time varying using BART methods as in [Pratola, et al. \(2020\)](#). But our factor-BART VAR already exhibits a high degree of flexibility.

References

- Adrian, Tobias, Nina Boyarchenko, and Domenico Giannone (2019), “Vulnerable growth,” *American Economic Review*, 109, 1263–89, <https://doi.org/10.1257/aer.20161923>.
- Angrist, Joshua D., Oscar Jorda, and Guido M. Kuersteiner (2018), “Semiparametric estimates of monetary policy effects: String theory revisited,” *Journal of Business & Economic Statistics*, 36, 371–387, <https://doi.org/10.1080/07350015.2016.1204919>.
- Bai, Jushan, and Serena Ng (2007), “Determining the number of primitive shocks in factor models,” *Journal of Business & Economic Statistics*, 25, 52–60, <https://doi.org/10.1198/073500106000000413>.
- Bañbura, Marta, Domenico Giannone, and Lucrezia Reichlin (2010), “Large Bayesian vector auto regressions,” *Journal of Applied Econometrics*, 25, 71–92, <https://doi.org/10.1002/jae.1137>.
- Barnichon, Regis, and Christian Matthes (2018), “Functional approximation of impulse responses,” *Journal of Monetary Economics*, 99, 41–55, <https://doi.org/10.1016/j.jmoneco.2018.04.013>.
- Baumeister, Christiane, Pascal Frank, Florian Huber, and Gary Koop (2025), “Oil, inflation expectations, and household characteristics: A nonlinear heterogeneous agent var approach,” Mimeo, University of Notre Dame and University of Salzburg and University of Strathclyde.
- Baumeister, Christiane, and James D. Hamilton (2015), “Sign restrictions, structural vector autoregressions, and useful prior information,” *Econometrica*, 83, 1963–1999, <https://doi.org/10.3982/ECTA12356>.
- Carriero, Andrea, Todd E. Clark, and Massimiliano Marcellino (2019), “Large Bayesian vector autoregressions with stochastic volatility and non-conjugate priors,” *Journal of Econometrics*, 212, 137–154, <https://doi.org/10.1016/j.jeconom.2019.04.024>.
- Carvalho, Carlos M, Nicholas G Polson, and James G Scott (2009), “Handling sparsity via the horseshoe,” in *Artificial intelligence and statistics*, 73–80, PMLR.
- Chan, Joshua C. C., Christian Matthes, and Xuwen Yu (2025), “Large structural VARs with multiple sign and ranking restrictions,” March, manuscript.
- Chan, Joshua C.C., Eric Eisenstat, and Rodney W. Strachan (2020), “Reducing the state space dimension in a large TVP-VAR,” *Journal of Econometrics*, 218, 105–118, <https://doi.org/10.1016/j.jeconom.2019.11.006>.
- Chauvet, Marcelle, and Jeremy Piger (2008), “A comparison of the real-time performance of business cycle dating methods,” *Journal of Business & Economic Statistics*, 26, 42–49, <https://doi.org/10.1198/073500107000000296>.
- Chipman, Hugh A., Edward I. George, and Robert E. McCulloch (2010), “BART: Bayesian additive regression trees,” *The Annals of Applied Statistics*, 4, 266–298, <https://doi.org/10.1214/09-AOAS285>.
- Clark, Todd E, Florian Huber, Gary Koop, Massimiliano Marcellino, and Michael Pfarrhofer (2023), “Tail forecasting with multivariate Bayesian additive regression trees,” *International Economic Review*, 64, 979–1022.
- Cogley, Timothy, and Thomas J Sargent (2005), “Drifts and volatilities: monetary policies and outcomes in the post wwii us,” *Review of Economic dynamics*, 8, 262–302.
- Crump, Richard K., Stefano Eusepi, Domenico Giannone, Eric Qian, and Argia Sbordone (2025), “A large Bayesian VAR of the United States economy,” *International Journal of Central Banking*, forthcoming.
- D’Agostino, Antonello, Luca Gambetti, and Domenico Giannone (2013), “Macroeconomic forecasting and structural change,” *Journal of Applied Econometrics*, 28, 82–101, <https://doi.org/https://doi.org/10.1002/jae.1257>.
- Favara, Giovanni, Simon Gilchrist, Kurt F. Lewis, and Egon Zakrajsek (2016), “Recession Risk and the Excess Bond Premium,” <https://doi.org/10.17016/2380-7172.1739>, FEDS Notes. Washington: Board of Governors of the Federal Reserve System, April 8, 2016.
- Forni, Mario, Luca Gambetti, Antonio Granese, Luca Sala, and Stefano Soccorsi (2025), “An American macroeconomic picture: Supply and demand shocks in the frequency domain,” *American Economic Journal: Macroeconomics*, 17, p. 311–341, <https://doi.org/10.1257/mac.20230295>.
- Gebetsberger, Manuel, Jakob W. Messner, Georg J. Mayr, and Achim Zeileis (2018), “Estimation methods for nonhomogeneous regression models: Minimum continuous ranked probability score versus maximum likelihood,” *Monthly Weather Review*, 146, 4323 – 4338, <https://doi.org/10.1175/MWR-D-17-0364.1>.

- Gilchrist, Simon, and Egon Zakrajšek (2012), “Credit spreads and business cycle fluctuations,” *American Economic Review*, 102, 1692–1720, <https://doi.org/10.1257/aer.102.4.1692>.
- Gonçalves, Sílvia, Ana María Herrera, Lutz Kilian, and Elena Pesavento (2024), “Nonparametric local projections.”
- Guerrón-Quintana, Pablo, Alexey Khazanov, and Molin Zhong (2023), “Financial and macroeconomic data through the lens of a nonlinear dynamic factor model,” *FEDS working paper*, <https://doi.org/10.17016/FEDS.2023.027>.
- Hauzenberger, Niko, Florian Huber, Karin Klieber, and Massimiliano Marcellino (2025), “Machine learning the macroeconomic effects of financial shocks,” *Economics Letters*, 250, p. 112260, <https://doi.org/https://doi.org/10.1016/j.econlet.2025.112260>.
- Huber, Florian, and Martin Feldkircher (2019), “Adaptive shrinkage in Bayesian vector autoregressive models,” *Journal of Business & Economic Statistics*, 37, 27–39.
- Huber, Florian, Gary Koop, Luca Onorante, Michael Pfarrhofer, and Josef Schreiner (2023), “Nowcasting in a pandemic using non-parametric mixed frequency vars,” *Journal of Econometrics*, 232, 52–69, <https://doi.org/https://doi.org/10.1016/j.jeconom.2020.11.006>.
- Huber, Florian, and Luca Rossini (2022), “Inference in Bayesian additive vector autoregressive tree models,” *The Annals of Applied Statistics*, 16, 104–123, <https://doi.org/10.1214/21-AOAS1488>.
- Kastner, Gregor (2019), “Sparse Bayesian time-varying covariance estimation in many dimensions,” *Journal of Econometrics*, 210, 98–115.
- Kim, Hee Soo, Christian Matthes, and Toàn Phan (2025), “Severe weather and the macroeconomy,” *American Economic Journal: Macroeconomics*, 17, p. 315–41, <https://doi.org/10.1257/mac.20220329>.
- Kolesár, Michal, and Mikkel Plagborg-Møller (2024), “Dynamic causal effects in a nonlinear world: the good, the bad, and the ugly,” *arXiv preprint arXiv:2411.10415*.
- Koop, Gary, M. Hashem Pesaran, and Simon M. Potter (1996), “Impulse response analysis in nonlinear multivariate models,” *Journal of Econometrics*, 74, 119–147, [https://doi.org/10.1016/0304-4076\(95\)01753-4](https://doi.org/10.1016/0304-4076(95)01753-4).
- Korobilis, Dimitris (2022), “A new algorithm for structural restrictions in Bayesian vector autoregressions,” *European Economic Review*, 148, p. 104241, <https://doi.org/https://doi.org/10.1016/j.euroecorev.2022.104241>.
- Makalic, Enes, and Daniel F. Schmidt (2015), “A simple sampler for the horseshoe estimator,” *IEEE Signal Processing Letters*, 23, 179–182, <https://doi.org/10.1109/LSP.2015.2503725>.
- McCracken, Michael W., and Serena Ng (2021), “FRED-QD: A Quarterly Database for Macroeconomic Research,” *Federal Reserve Bank of St. Louis Review*, 103, 1–44, <https://doi.org/10.20955/r.103.1-44>, First Quarter.
- Pratola, Matthew T., Hugh A. Chipman, Edward I. George, and Robert E. McCulloch (2020), “Heteroscedastic BART via multiplicative regression trees,” *Journal of Computational and Graphical Statistics*, 29, 405–417, <https://doi.org/10.1080/10618600.2019.1677243>.
- Primiceri, Giorgio E (2005), “Time varying structural vector autoregressions and monetary policy,” *The Review of Economic Studies*, 72, 821–852, <https://doi.org/10.1111/j.1467-937x.2005.00353.x>.
- Sims, Christopher A, and Tao Zha (2006), “Were there regime switches in us monetary policy?” *American Economic Review*, 96, 54–81.
- Velasco, Sofia (2025), “Let the Tree Decide: FABART A Non-Parametric Factor Model.”
- Waghmare, Kartik, and Johanna Ziegel (2025), “Proper scoring rules for estimation and forecast evaluation,” *arXiv preprint arXiv:2504.01781*.

Online Appendix

A Data Appendix

Table A.1: Overview of the dataset

Variable	Description	Transformation
GDPC1	Real Gross Domestic Product	5
PCECC96	Consumption	5
PRFIx	Residential fixed investment	5
PNFIx	Non-residential fixed investment	5
EXPGSC1	Exports	5
IMPGSC1	Imports	5
GCEC1	Government spending	5
surplus%gdp	Federal surplus (%nominal GDP)	1
FGRECPTx	Federal tax receipts	5
GDPCTPI	GDP price index	6
PCECTPI	PCE price index	6
PCEPILFE	Core PCE price index	6
CPIAUCSL	CPI	6
CPILFESL	Core CPI	6
HRLYCOMP	Hourly compensation	6
OPHNFB	Labor productivity	5
dtfp_util	Utilization-adjusted TFP	1
PAYEMS	Payroll employment	5
UNRATE	Unemployment rate	2
INDPRO	Industrial production	5
CUMFNS	Capacity utilization (manuf.)	1
HOUST	Housing starts	5
DPIC96	Disposable income	5
UMCSENTx	Consumer sentiment	1
FEDFUNDS	Federal funds rate	2
TB3MS	3-month T-bill rate	2
GS2	2-year Treasury yield	2
GS5	5-year Treasury yield	2
GS10	10-year Treasury yield	2
PRIMERATE	Prime loan rate	2
AAA	AAA corporate yield	2
BAA	BAA corporate yield	2
TWEXAFEGSMTHx	Exchange rate index	5
SP500	S&P 500	5
OILPRICEx	Spot price of oil	6

Notes: The time series are sourced from the McCracken & Ng database. The transformation codes mean: 1 = raw series, 2 = differences, 3 differences of differences, 4 = logarithm, 5= log differences, 6= differences of log differences.

B Technical Appendix

Details on the Full Conditional Posterior Distributions

The following section provides more details on the full conditional posterior distributions required for posterior simulation of the factor-BART VAR model.

- **Sampling the VAR coefficients \mathbf{A} :** Let \mathbf{a}'_s denote the s^{th} row of the coefficient matrix \mathbf{A} . Conditional on all other model parameters and latent states, \mathbf{a}_s follows a Gaussian distribution:

$$\mathbf{a}_s \mid \bullet \sim \mathcal{N}(\bar{\mathbf{a}}_s, \bar{\mathbf{V}}_s),$$

with

$$\bar{\mathbf{V}}_s = \left(\frac{\mathbf{X}'\mathbf{X}}{\omega_s^2} + \mathbf{D}_{a,s}^{-1} \right)^{-1}, \quad \bar{\mathbf{a}}_s = \bar{\mathbf{V}}_s \left(\frac{\mathbf{X}'}{\omega_s^2} (\mathbf{Y}_s - \mathbf{F}\boldsymbol{\lambda}_{f,s} - \mathbf{Q}\boldsymbol{\lambda}_{q,s}) + \mathbf{D}_{a,s}^{-1}\underline{\mathbf{a}}_s \right).$$

Here, \mathbf{X} is a $T \times K$ matrix that stacks the regressors \mathbf{x}_t , and \mathbf{Y}_s is a $T \times 1$ vector stacking the dependent variable y_{st} over time. The matrix $\mathbf{D}_{a,s}$ is diagonal with entries $\psi_{a,sj}^2 \tau_a^2$, and $\underline{\mathbf{a}}_s$ is the Horseshoe prior mean. The matrices \mathbf{F} and \mathbf{Q} stack the latent nonlinear factors \mathbf{f}_t and innovation factors \mathbf{q}_t , respectively.

- **Factor Loadings $\boldsymbol{\Lambda}_f$ and $\boldsymbol{\Lambda}_q$:** Each row of the factor loading matrices is sampled independently. For $\boldsymbol{\lambda}_{f,s}$, the conditional posterior is:

$$\boldsymbol{\lambda}_{f,s} \sim \mathcal{N}(\bar{\boldsymbol{\lambda}}_{f,s}, \bar{\mathbf{V}}_{f,s}),$$

with

$$\bar{\mathbf{V}}_{f,s} = \left(\frac{\mathbf{F}'\mathbf{F}}{\omega_s^2} + \mathbf{D}_{f,s}^{-1} \right)^{-1}, \quad \bar{\boldsymbol{\lambda}}_{f,s} = \bar{\mathbf{V}}_{f,s} \left(\frac{\mathbf{F}'}{\omega_s^2} (\mathbf{Y}_s - \mathbf{X}\mathbf{a}_s - \mathbf{Q}\boldsymbol{\lambda}_{q,s}) \right),$$

where $\mathbf{D}_{f,s}$ is a diagonal matrix with entries $\psi_{f,sj}^2 \tau_{f,s}^2$ and \mathbf{F} is a $T \times Q_f$ matrix stacking \mathbf{f}_t .

For $\boldsymbol{\lambda}_{q,s}$, we have:

$$\boldsymbol{\lambda}_{q,s} \sim \mathcal{N}(\bar{\boldsymbol{\lambda}}_{q,s}, \bar{\mathbf{V}}_{q,s}),$$

with

$$\bar{\mathbf{V}}_{q,s} = \left(\frac{\mathbf{Q}'\mathbf{Q}}{\omega_s^2} + \frac{1}{100}\mathbf{I} \right)^{-1}, \quad \bar{\boldsymbol{\lambda}}_{q,s} = \bar{\mathbf{V}}_{q,s} \left(\frac{\mathbf{Q}'}{\omega_s^2} (\mathbf{Y}_s - \mathbf{X}\mathbf{a}_s - \mathbf{F}\boldsymbol{\lambda}_{f,s}) \right),$$

where \mathbf{Q} is a $T \times Q_q$ matrix stacking \mathbf{q}_t .

- **Nonlinear Factors \mathbf{f}_t :** Given $\boldsymbol{\Lambda}_f$ and all other parameters, the nonlinear factors follow:

$$\mathbf{f}_t \sim \mathcal{N}(\bar{\mathbf{f}}_t, \bar{\mathbf{V}}_f),$$

with

$$\bar{\mathbf{V}}_f = (\boldsymbol{\Lambda}_f' \boldsymbol{\Omega}^{-1} \boldsymbol{\Lambda}_f + \mathbf{V}_f^{-1})^{-1}, \quad \bar{\mathbf{f}}_t = \bar{\mathbf{V}}_f (\boldsymbol{\Lambda}_f' \boldsymbol{\Omega}^{-1} (\mathbf{y}_t - \mathbf{A}\mathbf{x}_t) + \mathbf{V}_f^{-1} \boldsymbol{\mu}(\mathbf{x}_t)).$$

- **Static factors \mathbf{q}_t :** The innovation factors are drawn from:

$$\mathbf{q}_t \sim \mathcal{N}(\bar{\mathbf{q}}_t, \bar{\mathbf{V}}_q),$$

with

$$\bar{\mathbf{V}}_q = (\boldsymbol{\Lambda}_q' \boldsymbol{\Omega}^{-1} \boldsymbol{\Lambda}_q + \mathbf{V}_q^{-1})^{-1}, \quad \bar{\mathbf{q}}_t = \bar{\mathbf{V}}_q (\boldsymbol{\Lambda}_q' \boldsymbol{\Omega}^{-1} (\mathbf{y}_t - \mathbf{A}\mathbf{x}_t - \boldsymbol{\Lambda}_f \mathbf{f}_t)).$$

- **Tree structures and terminal node parameters:** Each function is updated via Bayesian backfitting as in [Chipman, George, and McCulloch \(2010\)](#). Conditional on $\{f_{jt}\}_{t=1}^T$, each function $\mu_j(\mathbf{x}_t)$ is approximated by a sum-of-trees model. Each tree is updated based on residuals obtained by subtracting the contribution of all other trees. Conditional on the trees we sample the terminal node parameters from independent univariate Gaussian distributions.
- **Error Variances $\boldsymbol{\Omega}$ and \mathbf{V}_q :** For each $s = 1, \dots, M$, the posterior for the diagonal

elements of $\boldsymbol{\Omega}$ is:

$$\omega_s^2 \sim \mathcal{IG} \left(a_\omega + \frac{T}{2}, b_\omega + \frac{1}{2} \sum_{t=1}^T (y_{st} - \hat{y}_{st})^2 \right),$$

where $\hat{y}_{st} = \mathbf{a}'_s \mathbf{x}_t + \boldsymbol{\lambda}'_{f,s} \mathbf{f}_t + \boldsymbol{\lambda}'_{q,s} \mathbf{q}_t$.

For each $j = 1, \dots, Q_q$, the posterior for the diagonal elements of \mathbf{V}_q is:

$$v_{q,jj} \sim \mathcal{IG} \left(a_q + \frac{T}{2}, b_q + \frac{1}{2} \sum_{t=1}^T q_{jt}^2 \right).$$

- **Horseshoe Hyperparameters:** The global parameters τ_a , $\tau_{f,i}$ and local shrinkage parameters $\psi_{a,ij}$, $\psi_{f,ij}$ are sampled using the efficient sampler of [Makalic and Schmidt \(2015\)](#).

C Additional Empirical Results

		(a) LPL			(b) CRPS		
		$h =$			$h =$		
	$Q_f \downarrow$	1	4	8	1	4	8
Output and Labor Markets							
GDPC1	3	-0.02	-0.02	0.00	1.02	1.02	1.01
	6	-0.05	-0.03	-0.02	1.04	1.03	1.03
	12	-0.01	-0.05	-0.00	1.01	1.02	1.01
INDPRO	3	-0.01	-0.01	0.00	1.01	1.01	1.00
	6	-0.01	-0.01	-0.01	1.01	1.00	1.00
	12	0.03	0.02	0.04	0.97	0.98	0.97
UNRATE	3	0.00	0.42	-1.88	1.00	1.00	1.00
	6	-0.01	2.00	-0.90	1.01	1.00	1.00
	12	0.01	-0.19	2.04	0.99	1.00	0.99
Prices							
GDPCTPI	3	0.02	0.03	0.03	0.99	0.99	0.99
	6	0.22	0.19	0.16	0.88	0.90	0.91
	12	0.14	0.10	0.10	0.92	0.95	0.94
PCECTPI	3	0.04	0.04	0.04	0.98	0.97	0.98
	6	0.31	0.29	0.28	0.82	0.82	0.82
	12	0.21	0.16	0.20	0.87	0.90	0.87
PCEPILFE	3	0.02	0.02	0.02	0.99	0.99	0.99
	6	0.21	0.16	0.16	0.86	0.89	0.90
	12	0.14	0.07	0.09	0.91	0.95	0.94
CPIAUCSL	3	0.04	0.04	0.03	0.98	0.98	0.98
	6	0.25	0.26	0.26	0.85	0.84	0.83
	12	0.18	0.15	0.20	0.89	0.91	0.87
CPILFESL	3	-0.00	0.01	0.02	1.01	0.99	0.99
	6	-0.08	0.10	0.13	1.08	0.92	0.90
	12	-0.09	0.08	0.14	1.08	0.92	0.89
Interest rates							
GS2	3	0.03	0.02	0.01	0.98	0.98	0.99
	6	-0.09	-0.08	-0.07	1.08	1.07	1.06
	12	-0.11	-0.10	-0.10	1.10	1.09	1.09
Joint log predictive likelihood							
	3	7.22	-0.73	-7.21			
	6	7.07	-7.03	1.69			
	12	0.63	1.29	1.14			

Notes: The table shows forecast losses relative to the VAR. Panel (a) shows the differences in log predictive likelihood while panel (b) shows the continuous ranked probability score. Joint refers to the joint predictive likelihood over the focus variables we consider in this table.

Table C.1: Average log predictive likelihoods and continuous ranked probability scores to the VAR over the hold-out period: Sample through 2019:Q4